

# African Journal of Pure and Applied Chemistry

volume 9 Number 8 August 2015

ISSN 1996-0840



*Academic  
Journals*

## ABOUT AJPAC

The **African Journal of Pure and Applied Chemistry (AJPAC)** is an open access journal that publishes research analysis and inquiry into issues of importance to the science community. Articles in AJPAC examine emerging trends and concerns in the areas of theoretical chemistry (quantum chemistry), supramolecular and macromolecular chemistry, relationships between chemistry and environment, and chemicals and medicine, organometallic compounds and complexes, chemical synthesis and properties, chemicals and biological matters, polymer synthesis and properties, nanomaterials and nanosystems, electrochemistry and biosensors, chemistry and industry, chemistry and biomaterials, advances in chemical analysis, instrumentation, speciation, bioavailability. The goal of AJPAC is to broaden the knowledge of scientists and academicians by promoting free access and provide valuable insight to chemistry-related information, research and ideas. AJPAC is a bimonthly publication and all articles are peer-reviewed.

**African Journal of Pure and Applied Chemistry (AJPAC)** is published twice a month (one volume per year) by Academic Journals.

### Contact Us

**Editorial Office:** [ajpac@academicjournals.org](mailto:ajpac@academicjournals.org)

**Help Desk:** [helpdesk@academicjournals.org](mailto:helpdesk@academicjournals.org)

**Website:** <http://www.academicjournals.org/journal/AJPAC>

**Submit manuscript online** <http://ms.academicjournals.me/>.

## Editors

**Prof. Tebello Nyokong**

*Acting Editor  
Chemistry Department  
Rhodes University  
Grahamstown 6140,  
South Africa.*

**Prof. F. Tafesse**

*Associate Editor  
Associate professor  
Inorganic chemistry  
University of South Africa  
South Africa.*

## Editorial Board

**Dr. Fatima Ahmed Al-Qadri**

*Asst. Professor  
Chemistry Department  
Sana'a University  
Republic of Yemen.*

**Dr. Aida El-Azzouny**

*National Research Center  
(NRC, Pharmaceutical and  
Drug Industries Research Division)  
Dokki-Cairo, 12622-Egypt.*

**Dr. Santosh Bahadur Singh**

*Department of Chemistry  
University of Allahabad  
Allahabad, India.*

**Dr. Gökhan Gece**

*Department of Chemistry  
Bursa Technical University  
Bursa, Turkey.*

**Dr. Francisco Torrens**

*Institute for Molecular Science  
University of Valencia  
Paterna Building Institutes  
P. O. Box 22085  
E-46071 Valencia  
Spain.*

**Dr. Erum Shoeb**

*Asst. Professor  
Department of Genetics  
University of Karachi  
Karachi-75270  
Pakistan.*

**Dr. Ishaat Mohammad Khan**

*Physical Research Laboratory  
Department of Chemistry  
Aligarh Muslim University  
Aligarh 202002, India.*

**Prof. Jean-Claude Bunzli**

*Department of Chemistry  
Swiss Federal Institute of Technology Lausanne  
(EPFL)  
Institute of Chemical Sciences and Engineering  
BCH 1402  
CH-1015 Lausanne (Switzerland).*

**Mrinmoy Chakrabarti**

*Department of Chemistry,  
Texas A&M University  
415 Nagle Street, College Station, TX 77840  
USA.*

**Dr. Geoffrey Akien**

*430 Eisenhower Drive, Apartment B-2,  
Lawrence, Kansas 66049,  
United States.*

**Prof. Anil Srivastava**

*Jubilant Chemsys Ltd.,  
B-34, Sector-58,  
Noida 201301 (UP),  
India.*

## ARTICLES

### Research Articles

- Nutritional and anti-nutritional composition of date palm (*Phoenix dactylifera L.*) fruits sold in major markets of Minna Niger State, Nigeria**  
E. Y. Shaba, M. M. Ndamitso, J. T. Mathew, M. B. Etsunyakpa, A. N. Tsado and S. S Muhammad **167**
- Spectrophotometric study on the stability constants and thermodynamic parameters of Zn<sup>2+</sup>, Cd<sup>2+</sup> and Hg<sup>2+</sup> complexes with Imino Thiazolidinone**  
Zewdu B. Gemechu, Tesfahun Kebede, Ephrem G. Demissie, Girma W. Woyessa and Solomon B. Kassa **175**
- Thermodynamic analysis of some volatile species at elevated pressure and temperature during combustion of Pakistani Lakhra and Thar lignite chars**  
Gul-e-Rana Jaffri, Syed Ali Rizwan shah Jaffri and Syed Ali Rehan Shah Jaffri **184**

Full Length Research Paper

## Nutritional and anti-nutritional composition of date palm (*Phoenix dactylifera* L.) fruits sold in major markets of Minna Niger State, Nigeria

E. Y. Shaba\*, M. M. Ndamitso, J. T. Mathew, M. B. Etsunyakpa, A. N. Tsado and S. S Muhammad

Department of Chemistry Federal University of Technology, Minna, P.M.B 65, Minna, Niger State, Nigeria.

Received 10 July, 2015; Accepted 18 August, 2015

This study investigated the nutritional, anti-nutritional factors, functional properties, mineral and amino acid contents of *Phoenix dactylifera* L. fruits using standard analytical methods. The results revealed that date palm (*P. dactylifera* L.) contain some percentage crude protein ( $1.21 \pm 0.02\%$ ), crude fat ( $1.73 \pm 0.46\%$ ), crude fibre ( $2.26 \pm 0.07\%$ ), ash ( $1.88 \pm 0.03\%$ ), moisture contents ( $1.16 \pm 0.16\%$ ), carbohydrate ( $91.76 \pm 0.06\%$ ), and calorific values ( $1621.50 \pm 0.12$  kg/100 g) respectively. The anti-nutrient composition for oxalate, tannins, saponins, alkaloids, cyanide, and flavonoids were  $7.57 \pm 0.04$ ,  $5.25 \pm 0.04$ ,  $1.89 \pm 0.12$ ,  $5.20 \pm 0.46$ ,  $0.80 \pm 0.01$  and  $34.29 \pm 3.49\%$  respectively; these result indicated that the sample is free of toxic substance which might cause harm to the body. The non-essential amino acids which give rise to about 62% make the plant more desirable since non-essential amino acid play important role in the body structure of a human. Though, both essential and non-essential amino acid present were there to complement each other. The elemental analysis of the fruit in mg/kg indicated that the fruit contained appreciable levels of K (11105 mg/kg), Na (913 mg/kg), Mg (799 mg/kg) and P (793 mg/kg). This showed that the fruit can serve as good source of minerals.

**Key words:** Nutritional, anti-nutritional, functional, mineral composition.

### INTRODUCTION

The date palm (*Phoenix dactylifera* L.) plays an important social, environmental, and economic role for many people living in arid and semiarid regions of the world. Fruits of the date palm are very commonly consumed in many parts of the world and considered as a vital component of the diet and a staple food in most Arab countries (Al-Farsi and Lee, 2008). It may be one of the oldest cultivated plants, with a history of more than 6000

years. The world production of dates has increased from about 4.6 million tons in 1994 to 7.68 million tons in 2010, with expectations of continuous increase (Al-Farsi and Lee, 2008). Nearly 2000 cultivars of date palm are known in the world, but only some have been evaluated for their performance and fruit quality. The importance of fruits as a source of nutrient has attracted attention of various researchers throughout the world, especially in Nigeria

\*Corresponding author. E-mail: [chimistzionist@yahoo.com](mailto:chimistzionist@yahoo.com)

Author(s) agree that this article remain permanently open access under the terms of the [Creative Commons Attribution License 4.0 International License](http://creativecommons.org/licenses/by/4.0/)

(Anhwange et al., 2004; Hassan and Umar, 2004; Umar et al., 2007). Malnutrition is a major health problem in Africa, despite government's efforts to promote food production. Protein-energy malnutrition in infants and children is one of the most common nutritional problems (Achu, 2004). Date palm (*P. dactylifera* L.) belongs to the Palmae (Arecaceae) family. The date palm is a palm broadly developed for its palatable organic product (Rani et al., 2007). The products of the date palm (*P. dactylifera* L.) are sweet berries with a sugar substance of more than half. Regularly, this palm developed for nearby markets on little land possessions other than other. In light of its high nourishing worth, extraordinary yields and its long life the date palm has been specified as the "tree of life" (Augstburger et al., 2002). It contains abnormal state of sugar substance, vital vitamins and high supplement thickness. In perspective of the present rate of populace development in creating nations, date palm natural product may be more valuable in some sustenance definitions than for direct utilization in the wake of cooking/simmered. The use of any seed as a source of nutritious food arises from the knowledge of the chemical composition of its flour and other products (Ogungbenle, 2011).

## MATERIALS AND METHODS

### Collection and preparation of plant sample

The fruits were collected from different market namely Bosso, Maikunkere, Mobil and Kure market. Niger State, Nigeria. The sample was collected in month of June, 2013. The fruits were thoroughly washed with distilled water and air dried at room temperature. These were then grind into uniform powder manually and stored in air tight containers prior to the commencement of the analysis.

### Proximate analysis

The standard analytical procedures for food analysis were adopted for the determination of the moisture content, crude protein, crude fibre, percentage lipids, carbohydrate, ash and calorific value.

#### Determination of moisture content

Two grammes of the sample were put into the crucibles, dried in an oven at 105°C overnight. The dried sample was cooled in a desiccator for 30 min and weighed to a constant weight. The percentage loss in weight was expressed as percentage moisture content on dry weight basis (AOAC, 2006). This was repeated three times to obtain triplicate values.

#### Determination of ash content

From the dried and ground sample, 2.00 g was taken in triplicates and placed in pre-weighed crucibles and ashed in a muffle furnace at 600°C for 3 h. The hot crucibles were cooled in a desiccator and weighed. The percentage residual weight was expressed as ash content (AOAC, 2006).

### Crude lipid content determination

From the pulverized sample, 2.00 g was used for determining the crude lipid by extracting the lipid from it for 5 h with (60 to 80°C) petroleum ether in a soxhlet extractor (AOAC, 2006). Triplicate samples were extracted to obtain triplicate values that were later averaged.

### Protein determination

Total protein was determined by the Kjeldahl method. 0.5 g of the sample was weighed in triplicate into a filter paper and put into a Kjeldahl flask, 8 to 10 cm<sup>3</sup> of concentrated H<sub>2</sub>SO<sub>4</sub> were added and then digested in a fume cupboard until the solution became colourless. Distillation was carried out with about 10 cm<sup>3</sup> of 40% NaOH solution. The condenser tip was dipped into a conical flask containing 5 cm<sup>3</sup> of 4% boric acid in a mixed indicator till the boric acid solution turned green. Titration was done in the receiver flask with 0.01 M HCl until the solution turned red (AOAC, 2006).

### Determination of crude fibre

From the pounded sample, 2.00 g were used in triplicates for estimating the crude fibre by acid and alkaline digestion methods using 20% H<sub>2</sub>SO<sub>4</sub> and 20% NaOH solutions (AOAC, 2006).

### Carbohydrate determination

The carbohydrate content was calculated using the following formula: Available carbohydrate (%), = 100 - [protein (%) + Moisture (%) + Ash (%) + Fibre (%) + Crude Fat (%)] (Mathew et al., 2014).

### Caloric value

The caloric value was calculated in kilocalories per 100 g (kcal/100 g) by multiplying the crude fat, protein and carbohydrate values by Atwater factors of 37, 17 and 17 respectively.

### Determination of mineral contents

The mineral elements were determined by the modification methods of Mathew et al. (2014), where sodium and potassium were determined using Gallenkamp Flame analyzer, while calcium, magnesium, iron, zinc and copper were determined using Buch Model 205 Atomic Absorption Spectrophotometer. Phosphorus level was determined using phosphovanado molybdate colorimetric techniques on JENWAY 6100 Spectrophotometer, blank (control) was also determined in the same manner.

### Functional properties

The standard analytical procedures for food analysis as described below were used.

#### Bulk density

Firstly, a dried and empty 10 cm<sup>3</sup> measuring cylinder was weighed. The sample was filled gently into the weighed 10 cm<sup>3</sup> measuring cylinder and then gently tapped at the bottom on a laboratory bench several times until there was no further diminution of the sample level after filling to the 10 cm<sup>3</sup> mark. After this, the filled measuring

cylinder was weighed and recorded. This process was repeated three times.

Calculation (AOAC, 2006):

$$\text{The bulk density (g/cm}^3\text{)} = \frac{\text{Weight of sample (g)}}{\text{Volume of sample (cm}^3\text{)}}$$

### pH measurement

The pH values of the samples were determined by suspending 10% W/V of the sample in distilled water in each case. It was then thoroughly mixed in a 100 cm<sup>3</sup> beaker, stirred and the pH was taken. This was repeated three times and the average calculated (Mathew et al., 2015).

### Water/oil absorption capacity

From the ground sample, 1.00 g was weighed into a conical graduated centrifuge tube and 10 cm<sup>3</sup> of water or oil was added to the weighed sample. A warring whirl mixer was used to mix the sample for 30 s. The sample was allowed to stand at room temperature for 30 min and then centrifuged at 5000 rpm for 30 min. After then the mixed sample was transferred from the graduated centrifuge tube into a 10 cm<sup>3</sup> measuring cylinder to know the volume of the free water or oil. The absorption capacity was expressed as grammes of oil or water absorbed per gramme of sample. Calculation; water/oil absorption capacity of the sample was calculated as: (Total oil/water absorbed - free oil/water) × Density of oil/water (AOAC, 2006).

### Foam capacity and stability

From the powdered sample, 2.00 g were weighed, blended with 100 cm<sup>3</sup> of distilled water using warring blender (Binatone BLG-555) and the suspension was whipped at 1600 rpm for 5 min. The mixture was then poured into a 100 cm<sup>3</sup> measuring cylinder and its volume was recorded after 30 s. Foam capacity was expressed as percent increase in volume using the formula of AOAC, (2006).

$$\text{Foam capacity} = \frac{\text{Volume after whipping} - \text{volume before whipping}}{\text{Volume before whipping}} \times 100$$

The foam stability of the sample was recorded at 15, 30, 60 and 120 s after whipping to determine the foam stability (FS).

$$\text{Foam stability} = \frac{\text{Foam volume after time}}{\text{Initial foam volume}} \times 100$$

### Gelatinization temperature

In triplicates, 5% sample was suspended in test tubes, heated in a boiling water bath with continuous stirring and 30 s after gelatinization was visually noticed, the temperature of the samples were taken as the gelatinization temperature (Mathew et al., 2015).

### Viscosity

In each case, 10% suspended sample in distilled water was taken and mechanically stirred for 2 h at room temperature. Thereafter, the viscosities of the samples were measured using Oswald type viscometer (AOAC, 2006).

### Emulsification capacity (EC)

From the sample, 2.00 g of sample were blended with 25 cm<sup>3</sup> of distilled water at room temperature for 30 s in a warring blender at 1600 rpm. After complete dispersion, 25 cm<sup>3</sup> of vegetable oil was gradually added and the blending continued for another 30 s. Then the mixture was transferred into a centrifuge tube and centrifuged at 1600 rpm for 5 min. The volume of oil separated from the sample was read directly from the tube after centrifuging. Calculation: The emulsion capacity was expressed as the amount of oil emulsified and held per gramme of sample:

$$\text{Emulsion capacity} = \frac{X}{Y} \times 100$$

Where X = height of emulsified layer and Y = height of the whole solution in the centrifuge tube (AOAC, 2006).

### Wettability

Triplicate samples were weighed and in each case, 1.00 g was introduced into a 25 cm<sup>3</sup> measuring cylinder with a diameter of 1 cm and a finger was placed over the end of the cylinder. The mixture was inverted and clamped at a height of 10 cm from the surface of a 250 cm<sup>3</sup> beaker containing 100 cm<sup>3</sup> of distilled water. The finger was removed to allow the test material to be dumped. In this case, the wettability was taken as the time required for the sample to become completely wet (AOAC, 2006).

### Gelation capacity

In every case for triplicate samples, 5 cm<sup>3</sup> of 2-20% (w/v) suspended samples were in test tubes and heated for 1 h in a boiling water bath followed by rapid cooling under running cold tap water. The test tubes were further cooled for 2 h at 4°C and the gelation capacity was the least gelation concentration determined as the concentration when the sample from the inverted test tube did not fall or slip (AOAC, 2006).

### Quantitative determination of phytoconstituents

#### Determination of cyanide

The alkaline pictrate method of Onwuka (2005) was adopted. 5.0 g of sample was weighed each and dissolved in 50 cm<sup>3</sup> distilled water in corked conical flasks. The mixtures was allowed to stay overnight and then filtered. The extracts (filtrates) was collected, different concentration of hydrogen cyanic acid (HCN) was prepared containing 0.02 to 0.10 mg/ cm<sup>3</sup> cyanide. The absorbance of each was taken in a spectrophotometer at 490 nm and the cyanide standard curve was plotted. 1 cm<sup>3</sup> of each sample filtrate and standard cyanide solution was measured into three test tubes respectively and 4 cm<sup>3</sup> of alkaline pictrate solution was added to each and incubated in a water bath for 15 min. After colour development (reddish brown), the absorbance of each content in the test tubes was taken in a spectrophotometer at 490 nm against a blank containing only 1 cm<sup>3</sup> distilled water and 4 cm<sup>3</sup> alkaline pictrate solution (1 g of pictrate and 5 g of sodium carbonate (Na<sub>2</sub>CO<sub>3</sub>) were dissolved in a warm water in 200 cm<sup>3</sup> flasks and made up to 200 cm<sup>3</sup> with distilled water).

#### Determination of oxalate

A modification of the titrimetric method of Krishnaiah et al. (2009)



was used in the determination of oxalate in the frog meat samples. In this method, 75 cm<sup>3</sup> of 1.5 M H<sub>2</sub>SO<sub>4</sub> (made from 99% BDH AnalaR grade) was added to 1 g of the ground samples and the solution was carefully stirred intermittently with a magnetic stirrer for 60 minutes and filtered using Whatman No 1 filter paper after which 25 cm<sup>3</sup> of the filtrate was collected and titrated against hot (90°C) 0.1M KMnO<sub>4</sub> (BDH AnalaR grade) solution until a faint pink colour that persisted for 30 s appeared. This was repeated twice more and the concentration of oxalate in each sample was obtained from the calculation: 1 cm<sup>3</sup> of 0.1 M KMnO<sub>4</sub> = 0.006303 g Oxalate.

#### Determination of alkaloids

The quantitative determination of alkaloids was carried out by the alkaline precipitation through gravimetric method. Two grammes (2.00 g) of the sample was soaked in 20 cm<sup>3</sup> of 10% ethanolic acetic acid (BDH AnalaR grade). The mixture was allowed to stand for 4 h at room temperature. Thereafter, the mixture was filtered through Whatman filter paper no. 40. The filtrate (extract) was concentrated by evaporation over a steam bath to ¼th of its original volume. For the alkaloids to be precipitated, concentrated ammonia solution was added in drops to the extract until it was in excess. The resulting alkaloid precipitate was recovered by filtration using a previously weighed filter paper. After filtration, the precipitate was washed with 1% ammonia solution and dried in the oven at 60°C for 30 min, cooled in a desiccator and reweighed. The experiment was repeated two more times and the average was taken. The weight of alkaloids was determined by difference and expressed as a percentage of the weight of the sample analysed as shown.

$$\% \text{ Alkaloids} = \frac{w_2 - w_1}{\text{wt of sample}} \times 100$$

Where; w<sub>1</sub> = weight of filter paper and w<sub>2</sub> = weight of paper + alkaloid precipitated (Krishnaiah et al., 2009).

#### Determination of flavonoids

1 g of the sample was weighed and repeatedly extracted with 100 cm<sup>3</sup> of 80% methanol at room temperature. The mixture was then filtered through filter paper into a 250 cm<sup>3</sup> beaker and the filtrate was transferred into a water bath and allowed to evaporate to dryness and weighed. The % flavonoid was calculated using the formula:

$$x = \frac{w_2 - w_1}{w_3} \times 100$$

Where x = percentage flavonoids, w<sub>1</sub> = weight of empty beaker, w<sub>2</sub> = weight of empty beaker + flavonoid and w<sub>3</sub> = weight of sample (Krishnaiah et al., 2009).

#### Determination of saponin

0.5 g of the sample was added to 20 cm<sup>3</sup> of 1M HCl and was boiled for 4 h. After cooling it was filtered and 50 cm<sup>3</sup> of petroleum ether was added to the filtrate and the ether layer evaporated to dryness. 5 cm<sup>3</sup> of acetone/ethanol mixture was added to the residue. 0.4 cm<sup>3</sup> of each was taken into 3 different test tubes. 6 cm<sup>3</sup> of ferrous sulphate reagent was added into them followed by 2 cm<sup>3</sup> of concentrated H<sub>2</sub>SO<sub>4</sub>. It was thoroughly mixed and after 10 min the absorbance was taken at 490 nm. Standard saponin was used to

establish the calibration curve (Krishnaiah et al., 2009).

#### Amino acid profile

The amino acid profile date palm sample was determined using methods described by Benitez (1989). From the ground sample, 0.50 g was defatted with chloroform and methanol mixture in a ratio of 1:1. Then, 0.25 g of the defatted sample was put into a glass ampoule, 7 cm<sup>3</sup> of 6 M HCl prepared from 36% BDH stock solution was added and oxygen expelled by passing nitrogen into the ampoule. This was put in the oven at 105°C for 22 h, allowed to cool and filtered. The filtrate was then evaporated to dryness at 40°C under vacuum in a rotary evaporator. The residue was dissolved with 5 cm<sup>3</sup> acetate buffer (pH 2.0) and loaded into the amino acid analyser and the samples were determined by ion exchange chromatographic (IEC) method using the Technicon Sequential Multi-sample Amino acid Analyzer (Technicon Instruments Corporation, New York).

## RESULTS AND DISCUSSION

Table 1 show the result of proximate composition of the proximate composition of date palm (*Phoenix dactylifera* L.). The result revealed that the moisture content in the sample was 1.16±0.16±0.16%. This value is lower than 5.24+0.05% and 11.0% reported by Ogungbenle (2011). The moisture content of different varieties of date palm as 14.81 ± 0.396 (Dora), 9.90 ± 0.042 (Dhaki), 12.3 ± 0.242 (Karbaline) respectively was reported by Faqir et al. (2012). The result of Rehman et al. (2012) also shows higher content of 17.70±0.03 for hard date palm. These differences may be due to the location, time, environments, longitivity and maturity of the sample used for the analysis. The low moisture content as saw in the sample is an evidence that this specimen may not be more inclined to decay, since nourishments with high dampness substance are more inclined to perishability (Fennema and Tannenbaum, 1996). It might be profitable in perspective of the specimen timeframe of realistic usability. This outcome is not shocking in perspective of the way that the advertisers of the item assert to the truth, that it can be put away for a year or more. The ash content of the sample was 1.88±0.03%. This result review that the sample have low ash content when compare to 3.27+0.02% by Ogungbenle (2011). These result is similar with 2.6 ± 0.12 reported by Gamal et al. (2012). This result is in agreement with the result obtained from the analysis of different varieties of date palm fruits 1.4 ± 0.171 for (Dora) , 1.9± 0.297 (Dhaki) and 1.6 ± 0.017 (Karbaline) respectively (Faqir et al., 2012). This result is within the acceptable ash content mean values of legumes of 2.4 to 5.0% recommended by FAO (1989). The result of the ash content in the sample is a suggestion of a low deposit of mineral elements in the samples compare to the recommended values by the FAO. This may indicate that date palm fruit would likely contain very high qualities essential minerals. Since ash content is an index to evaluate and grade the nutritive quality of foods (Pearson, 1976). Dietary fiber serves as a

**Table 1.** The proximate composition of date palm fruit.

Parameter	Values in % except for the calorific value
Moisture content	1.16±0.16
Ash content	1.88±0.03
Crude fibre	2.26±0.07
Crude protein	1.21±0.02
Fat (lipid)	1.73±0.04
Carbohydrate	91.76±0.06
Calorific value (kJ/100 g)	1621.50±0.12

The values are means of triplicate determinations ± standard deviations (SD).

**Table 2.** The anti-nutritional factors of date palm fruit.

Anti-nutritional factor	Concentration (%)
Oxalate	7.57±0.04
Tannin	5.25±0.04
Saponin	1.89±0.12
Alkaloid	5.20±0.40
Cyanide	0.80±0.01
Flavonoid	34.29±3.49

useful tool in the control of oxidative processes in food products and as functional food ingredient (Mandalari et al., 2010). The crude fibre content was 2.26±0.07% which is similar to 4.34±0.03% and 4.00±0.02 obtained by Ogungbenle (2011) and Rehman et al. (2012). This result is lower than 9.4 ± 0.10 reported by Gamal et al. (2012). Fibre content of foods helps in digestion process and prevention of cancer (Saldanha, 1995; UICC/WHO, 2005). Legumes are known to contain a percentage amount of fibre (Salunkhe et al., 1989). Crude fiber decreases the absorption of cholesterol from the gut in addition to delaying the digestion and conversion of starch to simple sugars, an important factor in the management of diabetes (Cust et al., 2009). The crude protein content of was 1.21±0.02% which is slightly lower than 2.1 ± 0.315 (Dora) 2.4 ± 0.052 (Dhaki) and 2.7 ± 0.187(Karbaline) respectively (Faqir et al., 2012). It has been reported that crude protein serves as enzymatic catalyst, mediate cell responses, control growth and cell differentiation (Whitney and Rolfes, 2005). Fat content of 1.73±0.04% was recorded from the analysis. The importance of lipids in food substances cannot be over-emphasized as it contributes significantly to the energy value of foods. The sample is so rich in carbohydrate (91.76±0.06%). The results showed that the date palm is a good source of carbohydrate which may give rise to good source of energy as an adult need about 400 to 500 g carbohydrate intake as starch. This value is slightly higher than 80.67±0.05 obtained Ogungbenle (2011). 1621.50±0.12 kJ/100 g calorific value was also recorded.

The nutritional importance of a given food depends on the nutrients and anti-nutritional constituents of the food (Aletor et al., 2007). The result of the anti-nutritional factors of date palm (*Phoenix dactylifera* L.) is presented in Table 2. The low value of 7.57±0.04% oxalate in the sample is evidence that utilization of date palm might not have any negative impact that is connected with abundance utilization of oxalate, for example, complex development with divalent metals, which may have impact on natural action of the metal particles in the body. Oxalate have been accounted for to have negative impact on accessibility of mineral which will prompt assimilation of fundamental minerals in body particularly calcium by framing insoluble salts (Onyeike and Omubode, 2002).The concentration of the value of saponins from the analysis was 1.89±0.12% which is within the WHO permissible limit of (48.50 mg/100 g) as recommended 2003 (WHO, 2003). The fruit contain 7.57% of tannin due to this result taking the fruit may not lower the availability of protein in the body or clothing with red blood cell as cause by excess tannin and saponins in human body. This suggests that this fruit may be safe for consumption. The fruit contain very low cyanide (0.80 %) which indicates that the fruit will not cause any effect as regard to cyanide. The flavonoid and alkaloid content was 34.29 and 5.20% respectively. The anti-nutritional composition of the sample was low. This indicates that the fruit can be used effectively since the anti-nutritional composition is low and there would be no interference with the nutrient like protein and minerals in the body.

**Table 3.** The functional properties of date palm fruit.

Parameter	Value
Bulk density (g/cm <sup>3</sup> )	0.67±0.02
pH	5.33±0.06
Water absorption capacity (%)	2.50±0.05
Oil absorption capacity (%)	1.22±0.10
Foam capacity (%)	5.15±1.07
Foam stability (%)	35.05±5.00
Emulsification capacity (%)	45.63±2.76
Gelation capacity (%)	16.67±1.16
Gelatinization temperature (°C)	72.01±0.60
Wettability (sec.)	7.37±0.45
Viscosity (sec.)	36.16±0.10

**Table 4.** The essential amino acid profile of date palm fruit.

Parameter	Concentration (g/100 g Protein)
Histidine	1.63±0.01
Isoleucine	1.85±0.10
Leucine	5.33±0.01
Lysine	2.50±0.03
Methionine	0.63±0.01
Threonine	1.25±0.05
Tryptophan	0.36±0.02
Valine	1.92±0.15
TEAA	37.18%

TEAA = Total essential amino acid.

The result of essential and non-essential amino acid profile of the date palm (*P. dactylifera* L.) were presented in Tables 4 and 5. The result showed that the essential amino acids content had higher Leucine (5.33±0.01) which is very useful in the body to counterbalance the isoleucine which help in the regulation of the thymus, spleen, pituitary, the metabolism and forming haemoglobin. The sample also had higher value of lysine (2.5±0.03) which helps in the functions of the liver, gallbladder and pineal and mammary glands. The sample contains histidine (1.63±0.01), isoleucine (1.85±0.10), threonine (1.25±0.05), valine (1.92±0.15), methionine (0.63±0.01), tryptophan (0.36±0.02) respectively. The presence of tryptophan, threonine, and valine is an indication that the plant can help in the generation of cells, red and white blood corpuscles, involved in the functioning of the mammary glands and ovaries. The major non-essential amino acid were glutamic acid (5.21±0.01), arginine (4.08±0.01), alanine (3.01±0.02), aspartic acid (3.37±0.02), phenylalanine (3.21±0.25), proline (2.02±0.01) and serine (2.35±0.12) respectively. The percentages of total essential and non-essential amino acid recorded in this work were 37.18 and 62,

respectively. The total percentage of essential amino acids (% TEAA) in the food samples was far above average, and this indicate that it may serve as good source of essential amino acids. Amino acids play central roles both as building blocks of proteins and as intermediates in metabolism. The consumption of this fruit can help reduce the effects associated with mal-nutrition.

The functional properties of the food materials are very important for the appropriateness of the diet, behavior of nutrients in food during processing, storage and preparation because they affect the general quality of foods as well as their acceptability (Omueti et al., 2009). The results of functional properties of date palm is presented in Table 3. Bulk density which is a function of particle size was 0.67±0.02 which is an indication that the particle size was high. Increase in bulk density is desirable because it offers greater packaging advantage, as a greater quantity may be packed within a constant volume (Fagbemi, 1999). The water absorption capacity was 2.50±0.05 indicating its heaviness, suggesting its suitability as a drug binder and disintegrate in pharmaceuticals industrials (Zaku et al., 2009). From

**Table 5.** The non-essential amino acid profile of date palm fruit.

Parameter	Concentration (g/100 g protein)
Alanine	3.01±0.02
Arginine	4.08±0.01
Aspartic acid	3.37±0.02
Cysteine	0.53±0.04
Glutamic acid	5.21±0.01
Glycine	1.07±0.01
Proline	2.02±0.01
Serine	2.35±0.12
Tyrosine	1.29±0.18
Phenylalanine	3.21±0.25
TNEAA	62%

TNEAA =Total non-essential amino acid.

**Table 6.** The mineral contents of date palm fruit.

Parameter	Concentration (mg/kg)
Sodium (Na)	913.00±1.00
Potassium (K)	11105.00±47.00
Calcium (Ca)	371.50±0.15
Magnesium (Mg)	799.50±4.50
Iron (Fe)	61.50±11.50
Zinc (Zn)	17.50±1.50
Manganese (Mn)	15.50±5.50
Copper (Cu)	10.00±0.16
Phosphorus	793.50±5.02

The values are mean of duplicate determination ± standard deviation (SD).

the table the result shows that the fruit had very higher gelatinization temperature of  $72.01 \pm 0.60^\circ\text{C}$  which affects the time required for the cooking of food substances. The result revealed very low value of oil absorption capacity of  $1.22 \pm 0.10\%$ . The pH of the sample was  $5.33 \pm 0.06$  has been reported by Tsakama et al. (2010) to increase solubility because of increased hydrophilic characters of the starch at these pH values. The pH value of  $5.33 \pm 0.06$  showed that this fruit is acidic in nature. The fruit contain Foam capacity ( $5.15 \pm 1.07\%$ ), foam stability ( $35.05 \pm 5.00\%$ ), emulsification capacity  $45.63 \pm 2.76\%$ , gelation capacity ( $16.67 \pm 1.16\%$ ), wettability ( $7.37 \pm 0.45$  s) and viscosity ( $36.16 \pm 0.10$  s) respectively.

Gelatinization includes the arrangement of a nonstop system which shows certain level of request. Gels are described by moderately high consistency, pliancy and flexibility. Gelation is one of the essential variables that focus starch practices in different sustenance and modern applications. It influences the nature of starch-based.

Table 6 shows that K, Na, Mg, P and Ca content of *P. dactylifera* fruit were  $11105 \pm 47.00$ ,  $913 \pm 1.00$ ,  $799.50 \pm 4.5$ ,  $793.50 \pm 5.02$  and  $371.50 \pm 0.15$  mg/kg respectively. Therefore, this fruit can serve as a good source of minerals that play significant roles in several biological processes.

## Conclusion

The detailed information on nutritional and health promoting components of *P. dactylifera* enhances our knowledge and appreciation for the use of date palm fruits in our daily diet and as a functional food ingredient. *P. dactylifera* fruits are characterized by high carbohydrate content and relatively reasonable amounts of K, Na, P, Mg and Ca. They are also rich in leucine, glutamic acid, argine, aspartic acid and alanine. Thus these fruits could be of high nutritional value serving as a good source of these nutrients for man and his animals.

**Conflict of Interest**

The authors have not declared any conflict of interest.

**REFERENCES**

- AOAC (Association of Official Analytical Chemists) (2006). Official Methods of Analysis, 15th edn. (Gaithersburg, S. edn). AOAC Press, Washington DC., USA. pp. 78- 90.
- Achu MB (2004). Preliminary nutritional evaluation of five species of egusi seeds in Cameroon. Afr. J. Food, Agric. Nutr. Dev. 4(1):43-48.
- Aletor O, Oshodin A, Ipinmoroti KO (2007). Comparative Evaluation of the Nutritive and Psysiochemical Characteristics of the leaves and leaf protein concentrates from two edible vegetables. J. Food Technol. 5(2):152-156.
- Anhwange BA, Ajibola VO, Oniye SJ (2004). Chemical Studies of the Seeds of *Moringa oleifera* and *Deuterium microcarpum*. J. Biol. Sci. 4 (6):711-715.
- Benitez LV (1989). Amino Acid and fatty acid profiles in aquaculture nutrition studies. pp. 23- 35. In S.S. De Silva (ed.) Fish Nutrition Research in Asia. Proceedings, of the Third Asian Fish Nutrition Network Meeting. Asian fish. Society Special Publication. 4:166. Asian Fisheries Society, Manila Philippines.
- Cust AE, Skilton MR, Van BMME (2009). Total dietary carbohydrate, sugar, starch and fibre intakes in the European Prospective Investigation into cancer and nutrition. Eur. J. Clin. Nutr. 63:37-60.
- Fagbemi TN (1999). Effect of blanching and ripening on functional properties of plantain (*Musa aab*) flour. Pts. Food Hum. Nutr. 54:261-269.
- Al-Farsi M, Lee CY (2008). Optimization of phenolics and dietary fibre extraction from date seeds. Food Chem. 108:977-985.
- Faqir MA, Sardar IB, Ahmad HE, Muhammad IK, Muhammad N, Shahzad H, Muhammad SA (2012). Phytochemical characteristics of Date Palm (*Phoenix dactylifera*) fruit extracts. Pak. J. Food sci. 22(3):117-127.
- Gamal AE, Salah MA, Mutlaq MA (2012). Nutritional Quality of Biscuit Supplemented with Wheat Bran and Date Palm Fruits (*Phoenix dactylifera* L.). Food Nutr. Sci. 3:322-328.
- Hassan LG, Umar KJ (2004). Proximate and Mineral Composition of Seeds and Pulp of African Locust Bean (*Parkia biglobosa*). Nig. J. Basic Appl. Sci. 13:15-27.
- Krishnaiah D, Devi T, Bono A, Sarbatly R (2009). Studies on phytochemical constituents of six Malaysian medicinal plants. J. Med. Plants Res. 3(2):67-72.
- Mandalari G, Tomaino A, Arcoraci T, Martorana M, Turco VL, Cacciola F, Rich GT, Bisignano C, Saija A, Dugo P, Cross KL, Parker ML, Waldron KW, Wickham MSJ (2010). Characterization of polyphenols, lipids and dietary fibre from almond skins (*Amygdalus communis* L.). J. Food. Comp. Anal. 23(2):166-174.
- Mathew JT, Ndamitso MM, Otori AA, Shaba EY, Inobeme A, Adamu A (2014). Proximate and Mineral Compositions of Seeds of Some Conventional and Non Conventional Fruits in Niger State, Nigeria. Acad. Res. Int. 5(2):113-118.
- Mathew JT, Ndamitso MM, Shaba EY, Mohammed SS, Salihu AB, Abu Y (2015). Determination of the Nutritive and Anti-Nutritive Values of *Pelophylax esculentus* (Edible Frog) Found in Hanyan Gwari, Minna Niger State, Nigeria. Adv. Res. 4(6):412-420.
- Omueti O, Bolanle O, Olayinka J Olukayode A (2009). Functional Properties of Complementary Diets Developed from Soybean (*Glycine max*), Groundnut (*Arachis hypogea*) and Crayfish (*Macrobrachium* spp.). Elect. J. Environ. Agric. Food Chem. 8(8):563 -573.
- Onwuka GI (2005). Food analysis and instrumentation theory and practice. Naphthali print, Nigeria. pp. 63-98.
- Onyeike EN, Omubo-Dede TT (2002). Effect of heat treatment on the proximate composition, energy values, and levels of some toxicants in African Yam bean (*Sphenostylis stenocarpa*) seed varieties. Plan. Foods Hum. Nutr. 57:223-231.
- Ogunbenle HN (2011). Chemical and fatty acid compositions of date palm fruit (*Phoenix dactylifera* L.). Flour. Bang. J. Sci. Ind. Res. 46(2):255-258.
- Rehman Z, Salariya AM, Zafar SI (2012). Effect of processing on available carbohydrate content and starch digestibility of kidney beans (*Phaseolus vulgaris* L.). Food Chem. 73:351-355.
- Rani CI, Kalaiselvi T, Jegadeeswari V (2007). The date palm. Accessed at [www.techno-preneur.net/information-desk/.../2007/.../Date\\_palm.pdf](http://www.techno-preneur.net/information-desk/.../2007/.../Date_palm.pdf).
- Saldanha LG (1995). Fibre in the diets of U.S. Children: Results of national surveys. Pediat. 96:994-996.
- Salunkhe DK, Kadam SS, Chavan JK (1989). CRC Postharvest Biotechnology of Food Legumes. CRC Press, Boca Raton, FL.
- Tsakama M, Mwangwela AM, Manani TA, Mahungu NM (2010). Physicochemical and pasting properties of starch extracted from eleven sweet potato varieties. Afr. J. Food Sci. Technol. 1(4):090-098.
- UICC/WHO (2005). Global Action Against Cancer NOW. Geneva: UICC and WHO Publications Department.
- Umar HA, Adamu R, Dahiru A, Nadro MS (2007). Level of Anti-nutritional factors in some wild edible fruits of Northern Nigeria. Afr. J. Biotechnol. 6(16):1935-1938.
- Whitney EN, Rolfes SR (2005). Understanding Nutrition. 10th Edition. Thomson /Wadsworth Publishing Company, Belmont, C. A. pp. 132-139.
- WHO (2003). Feeding and Nutrition of Infants and Young Children: Guidelines for the WHO European region with emphasis on the former Soviet Union. WHO Regional Publications, European Series. 87:1-296.
- Zaku SG, Aguzue OC, Thomas SA, Barminas JT (2009). Studies on the functional properties and the nutritive quality of amura plant starch (*Tacca involucrate*) a wild tropical plant. Afr. J. Food Sci. 3(10):320-322.

## Full Length Research Paper

# Spectrophotometric study on the stability constants and thermodynamic parameters of $Zn^{2+}$ , $Cd^{2+}$ and $Hg^{2+}$ complexes with Imino Thiazolidinone

Zewdu B. Gemechu, Tesfahun Kebede, Ephrem G. Demissie\*, Girma W. Woyessa and Solomon B. Kassa

Department of Chemistry, College of Natural and Computational Sciences, Haramaya University, Ethiopia.

Received 18 June, 2015; Accepted 21 July, 2015

The heterocyclic ligand (L), 3-(2-hydroxy phenyl)-2-iminothiazolidin-4-one, was synthesized by the cyclocondensation of o-hydroxy phenyl chloroacetamide with potassium thiocyanate. The stoichiometries of the title complexes were first determined by spectrophotometric mole ratio method which gave rise to the M:L ratio of 1:4 in case of Zn(II) and Cd(II) and 1:2 in case of Hg(II) ions respectively. Using these predetermined M:L ratios, complexes of the formulas  $[Zn-L_4]$ ,  $[Cd-L_4]$  and  $[Hg-L_2]$  were prepared accordingly using precursor of the corresponding metal salts with the title ligand in ethanol medium. The synthesized compounds were characterized by elemental analysis, FTIR,  $^1H$  and  $^{13}C$ NMR, UV-Vis and conductometric measurement. Stability constants ( $K_s$ ) of these complexes were investigated by spectrophotometric mole ratio method. The FTIR,  $^1H$  NMR and  $^{13}C$  NMR data revealed that the studied ligand function as monodentate ligand interacting through phenolic oxygen as donor with Zn(II) and Cd(II) and as bidentate ligand interacting through phenolic oxygen and nitrogen atom with Hg(II). The synthesized complexes show conductivity values in the range of 122-133  $\mu Smol^{-1}cm^2$  in DMSO at 298 K which confirms the electrolytic nature of the complexes. The stability constants decreased with increased temperature, confirming that these metal complexes are not stable at higher temperature. Sufficiently large negative values of  $\Delta G$  of complex confirm the spontaneous formation of the title complexes. Furthermore, it was noted that the spontaneity of the reaction increased with temperature. The stability constant of these complexes follow the sequence  $Zn(II) > Cd(II) > Hg(II)$ . Therefore, the overall result is complying very well with the Irving-William series of stability constants of metal complexes.

**Key words:** Stability constants, 3-(2-hydroxyphenyl)-2-iminothiazolidin-4-one, Irving-William series, thermodynamic parameters, mole ratio method.

## INTRODUCTION

Thiazolidinones are thiazolidine derivatives and have an atom of sulfur at position 1, an atom of nitrogen at

position 3 and a carbonyl group at position 2, 4 or 5. However, its derivatives belong to the most frequently

\*Corresponding author. E-mail: ephrem1977@gmail.com

Author(s) agree that this article remain permanently open access under the terms of the [Creative Commons Attribution License 4.0 International License](http://creativecommons.org/licenses/by/4.0/)

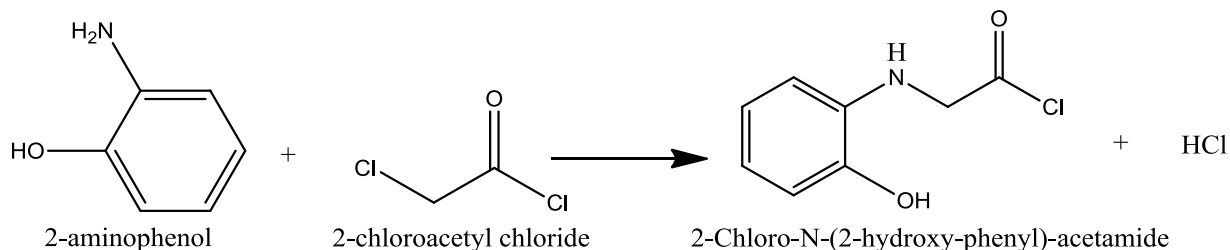


**Figure 1.** Synthesis of 2-Chloro-N-(2-hydroxy-phenyl)-acetamide.

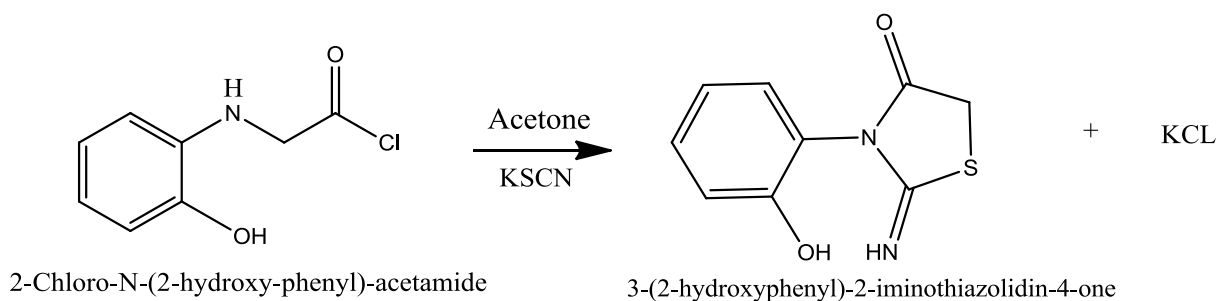


**Figure 2.** Synthesis of 3-(2-hydroxy phenyl)-2-iminothiazolidin-4-one.

studied moieties and its presence in penicillin was the first recognition of its occurrence in nature (Singh et al., 1981; Brown, 1961; Pulici and Quartieri, 2005). The perusal of literature shows that thiazolidine-4-ones have many interesting activity profiles, namely COX-1 inhibitors, inhibitors of the bacterial enzyme MurB, which was precursor acting during the biosynthesis of peptidoglycan, nonnucleoside inhibitors of HIV-RT and antihistaminic agents (Look et al., 1996; Andres et al., 2000; Barreca et al., 2001). Thiazolidinones are also known to exhibit antibacterial, anticonvulsant, antifungal, amoebicidal, antioxidant, and anticancer activities (Diurno et al., 1992; Mulwad and Choudhari, 2005.). Thiazolidine derivatives containing nitrogen oxygen and sulfur donors are being popular as biologically significant species. However a little known regarding on metal complexes of imino-derivatives of thiazolidinones of their complex equilibria, stability constant and physico-chemical properties of metal ion complexes. In this paper, we describe the syntheses, characterization, and thermodynamic parametres of synthesized thiazolidin-4-one with transition metal ions

## EXPERIMENTAL

### Synthesis of the ligand: 3-(2-hydroxy phenyl)-2-imino-1-thiazolidin-4-one

o-hydroxy phenyl chloro acetamide was prepared by 2-hydroxy aniline (0.05 mol) in ice cold benzene followed by 8 ml chloroacetyl

chloride added in 1 ml installments with vigorous stirring. Precipitate obtained was filtered out, washed with benzene, dried in air and crystallized by ethanol (Figure 1).

2-chloro-N-(2-hydroxyphenyl)-acetamide obtained from the previous reaction (5.986 g) and potassium thiocyanate (2.91 g) in acetone in 1:1 molar ratio were mixed, refluxed for 5 h and the product 3-(2-hydroxyphenyl)-2-iminothiazolidin-4-one was obtained as precipitate after evaporation of the solvent. Then the precipitate washed with water to ensure complete removal of unreacted KSCN and finally washed with dry acetone and ether successively. All the products were recrystallized from ethanol and dried in dry air and the purity was checked by TLC plates. Then, the air dried product was collected for further steps (Figure 2).

### Synthesis of the title complexes (M:L complex formation)

A common procedure was followed to prepare all complexes. To the solution containing 0.015 mol of each M (II) ions in hot ethanol, the ligand solution (0.015 mol) in ethanol was added with stirring and the reaction mixture was refluxed for about 2 h. The reaction product on cooling at room temperature yielded precipitate of the particular complexes. The precipitate obtained as such was then filtered, washed with water and ethanol successively and dried in air.

### Determination of stoichiometry (M:L ratio) of complexes by spectrophotometric mole ratio method

This method was used to determine the number of complexes formed and for choosing a wavelength suitable for performing further experiments. Absorption experiments were performed with mixtures containing varying molar ratios of reactants and number of maxima on the extrapolation of optical density and wavelength for each mixture set, were recorded to be informative of the number of

complexes formed in a given system. The wavelength obtained corresponding to wavelength maxima ( $\lambda_{\max}$ ) of a particular system was selected for use in all other spectrophotometric experiments (Vosburgh and Cooper, 1941). From the standard solutions, 2 ml of  $1.0 \times 10^{-2}$  M metal (II) chloride solutions were pipetted into each of eight 50 ml volumetric flasks and aliquots (2, 4, 6 to 16 ml) of  $1.0 \times 10^{-2}$  M ligand solution were mixed with thoroughly shaking the flasks to get homogenous solutions. Then, the absorbance was measured at maximum wavelength of each sample against reagent blank (DMSO) both at room temperature (that is, 25°C) and at 40°C.

### Test of purity of the compounds

#### Chloride test

From each complex, 30 mg was weighted and digested in nitric acid to remove organic content and diluted to give a clear solution to which  $\text{AgNO}_3$  solution was added in a drop wise manner. Absence of a white precipitate which could be due to  $\text{AgCl}$  in any of the complexes prepared indicates the absence of chlorine neither as chloride nor as coordinated chlorine.

#### TLC test

The purity of the complexes were tested by using thin-layer chromatography (TLC) on silica gel thin layers using two component solvent systems, ethyl acetate and n-hexane (9:1 ratio). A single spot on thin layer chromatogram was indicated that the complex was pure.

### Physico-chemical characterization

UV-visible spectra of the ligands and complexes were recorded on Varian Cary 500 spectrophotometer in the range 200 to 800 nm in solution. The IR spectra were recorded in KBr pellets (4000 to 400  $\text{cm}^{-1}$ ) on a Perkin-Elmer spectrum 2000 FT-IR spectrometer equipped with a DTG detector, in a region 4000 to 400  $\text{cm}^{-1}$ .  $^1\text{H}$  and  $^{13}\text{C}$ -NMR spectra were obtained on an Avance Bruker AMX 400 MHz spectrometer. All samples were prepared using deuterated solvents. Chemical shifts are reported in parts per million (ppm) relative to an internal standard tetramethylsilane (TMS).

## RESULTS AND DISCUSSION

### Electronic spectra and solvent effect on UV/Vis spectral of complexes

$\text{Zn}^{2+}$ ,  $\text{Cd}^{2+}$  and  $\text{Hg}^{2+}$  complexes are diamagnetic  $d^{10}$  ions and the electronic spectra of these complexes do not show any d-d transition band (Suresh and Prakash, 2010). The UV-Vis spectrum of the synthesized ligand is characterized mainly by one absorption band at 440 nm which may be assigned to  $n \rightarrow \pi^*$  transition. This transition was also observed in the spectra of the complexes, but with a red shift towards lower frequency, confirming the coordination of the ligand to the metal ions. The ligand as well as its metal complexes were found to be more soluble in DMSO, but only slightly soluble in methanol and ethanol. A series of solutions were prepared having a constant concentration ( $1 \times 10^{-2}$  M) of the metal ion but in

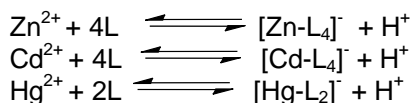
excess of these for the ligand so that the M:L ratios could be determined from the relationship between the absorption at  $\lambda_{\max}$  and the mole ratio obtained for each respective complex.

The UV/Vis absorption spectra of the iminothiazolidinone ligand and its complexes were obtained at room temperature in three organic solvents (Methanol, Ethanol and DMSO) with different polarity. In general, with increasing polarity of solvent the spectra of the ligand as well as the complex shifted to lower energy, that is, bathochromic shift observed. The solvent effect on the UV/Vis absorption spectra of the ligand (iminothiazolidinone (L) and its complexes ( $\text{Zn-L}_4$ ,  $\text{Cd-L}_4$  and  $\text{Hg-L}_2$ ) were found to be strongly dependent on the nature of the substituent on the imino group. This phenomenon may possibly be because by the difference in the conjugational or migrating ability of the lone pair electrons on nitrogen atoms of the ligand. These results are in accordance with structure of this ligand, such that the electronic behavior of the nitrogen atom of the amide group is somewhat different from carbonyl group as an electron-donating substituent.

### Stoichiometric studies and synthesis of metal ligand complexes

The stoichiometries of  $\text{Zn}^{2+}$ ,  $\text{Cd}^{2+}$  and  $\text{Hg}^{2+}$  complexes with the synthesized ligand were determined by the mole ratio method at constant metal ion concentration ( $1 \times 10^{-2}$  M) and varying ligand concentrations. The optical density of each complex solution was measured and the  $\lambda_{\max}$  occurs at 300, 305 and 295 nm in DMSO, respectively.

As shown in Figure 3, the intercepts of tangents on both arms of the graphs plotted between optical density and varying concentrations of ligand indicate 1:4, 1:4 and 1:2 metal to ligand interaction ratios of the complexes  $[\text{Zn-L}_4]$ ,  $[\text{Cd-L}_4]$  and  $[\text{Hg-L}_2]$ , respectively. The stoichiometric studies showed that there is a similar pattern of complexation with optical density (or absorbance) of each complex showing specific values at the two selected temperatures, that is, at 298 and 313K (Harvey and Manning, 1950). Therefore, results of the stoichiometric studies conducted on the prepared complexes using DMSO as a solvent suggested that the metal-ligand interactions may be expressed by the following complex equilibria forms:



### Thermodynamic parameters

The thermodynamic parameters were obtained spectrophotometrically by measuring the absorbance of



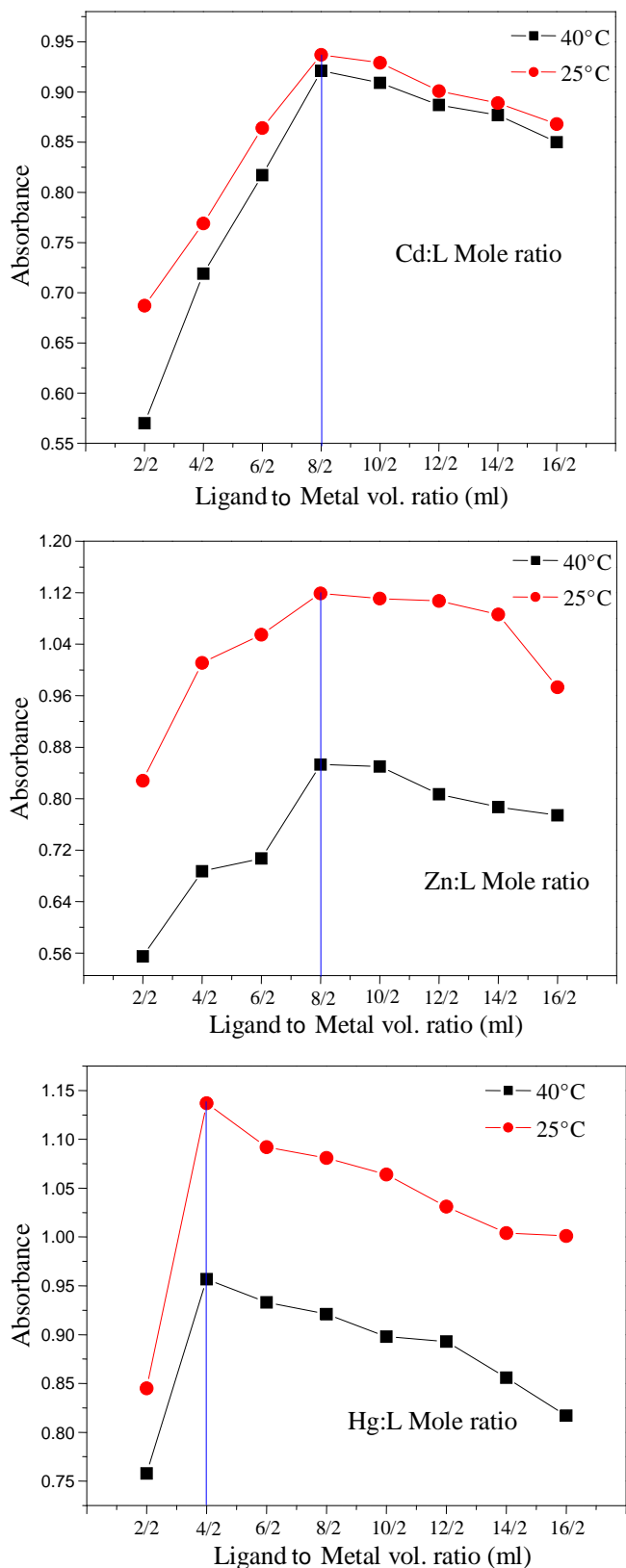


**Figure 3.** A graph plotted absorbance versus a function of VL/VM mole ratios of  $Zn^{2+}$ ,  $Cd^{2+}$  and  $Hg^{2+}$  complex with the ligand 3-(2-hydroxyphenyl)-2-iminothiazolidin-4-one at room (298 K) and 313 K temperatures.

solution of ligand and metal mixtures. The degree of formation of each complex was obtained according to the relationship indicated in Equations (1) and (2). The thermodynamic parameter of the metal ion complexes at five different temperatures 298, 303, 313, 323, 333 and 343 K were studied. The calculated  $\ln K_s$ ,  $\Delta G$ ,  $\Delta H$  and  $\Delta S$  values for the prepared complexes are recorded as follows:

$$\Delta G = -RT \ln K_s \quad (1)$$

$$\ln K_s = -\frac{\Delta H}{RT} + \frac{\Delta S}{R} \quad (2)$$

The value of  $\alpha$  (degree of dissociation) obtained by measuring the  $E_m$  (Maximum absorbance) and  $E_s$  (Absorbance found at correct Stoichiometry) from the maximum wavelength can be calculated using Equation 3.

$$\alpha = \frac{E_m - E_s}{E_m} \quad (3)$$

The free energies of formation ( $\Delta G$ ) of all metal complexes have negative values indicating spontaneity of the reaction process in all cases. In line with this, as the temperature increases, from 298 K to 343 K, the stability of complexes decreases.

### Effect of temperature

A perusal of data (Tables 2) shows that, the stability constant ( $K_s$ ) values decreases with an increase in temperature. Thus, higher temperature is not favorable for dissociation of proton from the carbonyl group of the ligand in these compounds implying that the values of metal-ligand stability constant decrease with increase in temperature. Thus, rise in temperature is not favorable for the formation stable complexes in these systems. As evidenced from Equation (2), the relationship between  $K_s$  and  $\Delta G$ , the values of free energies of formation of the complexes were become more and more negative with rise in temperature. This indicates that the complex formation is a spontaneous process and spontaneity increases with temperature. The observed entropy changes of the complex formation are positive in the range between 0.227 and 0.535  $\text{kJmol}^{-1}\text{K}^{-1}$ . Through the binding of ligand with the metal ions leads to more ordered system and this should lead to decrease entropy ( $-\Delta S$ ) yet the observed positive change in entropy may be due to the dissociation of ligand with ionic species that predominantly makes the net entropy change positive. As indicated in Table 1, the endothermic  $\Delta H$  values for all

**Table 1.** UV-Vis spectral data of Ligand and complexes in various solvents.

Solvents	Ligand $\lambda_{\text{max}}$ (nm)	[Zn-L <sub>4</sub> ] $\lambda_{\text{max}}$ (nm)	[Cd-L <sub>4</sub> ] $\lambda_{\text{max}}$ (nm)	[Hg-L <sub>2</sub> ] $\lambda_{\text{max}}$ (nm)
Methanol	280	246	241	234
Ethanol	278	237	233	230
DMSO	440	320	310	305

**Table 2.** Analytical data of metal-ligand stability constants, change in free energy, enthalpy and entropy of [Zn-L<sub>4</sub>], [Cd-L<sub>4</sub>] and [Hg-L<sub>2</sub>] complexes at various temperatures (298-343 K).

Temp (K)	$E_s$	$E_m$	$\alpha$	$\ln K_s$	$-\Delta G_0$ kJ/mol	$\Delta H$ kJ/mol	$\Delta S$ kJ/molK
<b>[Zn-L<sub>4</sub>]</b>							
298	2.066	2.174	0.049678	27.84	68.96	68.90	0.463
303	1.92	2.009	0.044301	28.41	71.58	71.52	0.472
313	1.86	1.925	0.033766	29.78	77.50	77.44	0.495
323	1.786	1.841	0.029875	30.40	81.63	81.57	0.505
333	1.722	1.764	0.02381	31.54	87.32	87.26	0.524
343	1.721	1.758	0.021047	32.16	91.71	91.65	0.535
<b>[Hg-L<sub>2</sub>]</b>							
298	1.95	2.397	0.186483	21.07	52.19	52.10	0.350
303	1.9	2.204	0.137931	22.63	57.01	56.92	0.376
313	1.84	2.035	0.095823	24.50	63.76	63.67	0.407
323	1.794	1.929	0.069984	26.10	70.09	70.00	0.434
333	1.752	1.838	0.04679	28.14	77.90	77.81	0.468
343	1.724	1.776	0.029279	30.50	86.98	86.89	0.507
<b>[Cd-L<sub>4</sub>]</b>							
298	2.063	2.386	0.135373	13.68	33.89	33.84	0.227
303	1.925	2.159	0.108384	14.38	36.21	36.16	0.239
313	1.851	2.009	0.078646	15.37	40.00	39.95	0.255
323	1.82	1.941	0.062339	16.09	43.20	43.15	0.267
333	1.759	1.841	0.044541	17.11	47.38	47.33	0.284
343	1.742	1.786	0.024636	18.91	53.93	53.87	0.314

L=3-(2-hydroxyphenyl)-2-iminothiazolidin-4-one.

complexes at the five different temperatures are comparable suggesting that, enthalpy is dependent on temperature in the given range (298 to 343 K). The variation in  $\Delta H$  values for all complexes provides clear evidence to the assumption that  $\Delta H$  value is dependent on the chemical structure of the complexes, that is, on strength of the M-L coordination. The observed positive entropy change and negative Gibbs energy change suggest that the complex formation is favored both by Gibbs energy as well as entropy gain. Therefore, based on the calculated values of thermodynamic parameters, order of stability of the title complexes is found to be [Zn-L<sub>4</sub>] > [Cd-L<sub>4</sub>] > [Hg-L<sub>2</sub>]. Thus, divalent Zn<sup>2+</sup> complex of imino thiazolidinone ligand has the highest value of stability constant. Generally, this order is found to be in good agreement with Irving-Williams order of stability.

## Elemental analysis

Physical properties and elemental analyses data of ligands and their complexes are presented in Tables 3 and 4. The proposed molecular formulae of the newly synthesized compounds are consistent with their analysis data of C, H, N, S and metal contents. For Zn<sup>2+</sup> and Cd<sup>2+</sup> complexes the metal-ligand ratios of 1:4 were established, whereas for Hg<sup>2+</sup> complex, 1:2 stoichiometry was recognized.

## Determination of metal contents by atomic absorption spectroscopy (AAS)

The atomic absorption spectroscopy (AAS) measurements

**Table 3.** Formula weight, % yield, melting point and elemental analyses data of the ligand and its complexes, with metals.

Compound	Mol. mass	% yield	Color	M.P ( $\pm 10^\circ\text{C}$ )	Elemental analysis calculated (experimental) %				
					C	H	N	S	M(II)
$\text{C}_9\text{H}_8\text{O}_2\text{N}_2\text{S}$	208.00	81	Pale yellow	120	51.92(51.87)	3.37(3.34)	13.46(13.39)	15.38(15.31)	-
[Zn-L <sub>4</sub> ]	893.38	74	Yellow	235	48.36(48.23)	3.13(3.08)	12.54(12.64)	14.33(14.21)	7.32(7.26)
[Cd-L <sub>4</sub> ]	940.41	77	White	244	45.94(45.44)	2.98(2.59)	11.91(12.01)	13.61(13.48)	11.95(11.88)
[Hg-L <sub>2</sub> ]	614.59	73	Yellowish brown	201	35.15(35.43)	2.28(2.34)	9.11(9.25)	10.41(10.28)	32.64(32.85)

L= 3-(2-hydroxyphenyl)-2-iminothiazolidin-4-one).

**Table 4.** FAAS analysis data for the metal-ligand complexes.

Complexes	Mol.wt	[M(II)] (ppm)	A	M(II) contents(%)	
				Calculated	Found
[Zn-L <sub>4</sub> ]	893.38	23.67	0.493	7.89	7.27
[Cd-L <sub>4</sub> ]	940.41	36.03	0.510	12.01	12.08

L= 3-(2-hydroxyphenyl)-2-iminothiazolidin-4-one; A = Absorbance.

**Table 5.** Observed IR frequencies ( $\text{cm}^{-1}$ ) of the ligand and its metal complexes.

Vibrational mode	$\text{C}_9\text{H}_8\text{O}_2\text{N}_2\text{S}$	[Zn-L <sub>4</sub> ]	[Cd-L <sub>4</sub> ]	[Hg-L <sub>2</sub> ]
$\nu\text{C}=\text{N}$	1547	1538	1546	1546
$\nu\text{C}=\text{O}$	1646	1638	1645	1645
$2^\circ$ amine $\nu\text{N}-\text{H}$	3383	3380	3382	3382
$\nu\text{C}-\text{N}$ ring	1371	1362	1371	1370
$\nu\text{C}-\text{S}$	639	626	638	638
Phenol $\nu\text{OH}$	3169	-	-	-
Phenol $\nu\text{C}-\text{O}$	1040	1030, 968, 1121	1041, 968, 1131	1040, 969, 1131
$\nu\text{C}=\text{C}$ Benz	1458, 1597	1587, 1450	1595, 1458	1595, 1458
$\nu\text{C}-\text{H}$ Arom	2979	3113	3116	3115
$\nu\text{M}-\text{O}$	-	587	578	446
$\nu\text{M}-\text{N}$	-	-	-	541

L= 3-(2-hydroxyphenyl)-2-iminothiazolidin-4-one).

on the synthesized complexes were conducted to know the metal contents and the results obtained were given in Table 4. The metal to ligand ratio for  $\text{Zn}^{+2}$  and  $\text{Cd}^{+2}$  complexes were found to be 1:4 and these coincide with the elemental analysis results.

### FTIR spectral analysis results

The IR data of the spectra for the Schiff base ligand and its metal complexes were presented in Table 5. Accordingly, the IR spectra of the complexes were compared with that of pure ligand in order to determine the coordination sites that could be involved in complex formation. The perusal of Table 5 reveals that absorption

bands corresponding to two weak bands at 2979 and 2929  $\text{cm}^{-1}$ , may be attributed to aromatic and aliphatic  $\nu(\text{C}-\text{H})$  peaks respectively. These showed very small red shift in position in all three chelate complexes. The spectra of the free ligand shows a strong peak at 3383  $\text{cm}^{-1}$ , which can be attributed to secondary  $\nu(\text{N}-\text{H})$  stretching vibration in the ligand and in all its complexes. Band of the free ligand at 1646  $\text{cm}^{-1}$ , assignable to stretching vibration due to  $\nu(\text{C}=\text{N})$  groups of imino thiazolidinone, did not shift in any of the complexes, suggesting that there was no involvement of the imine nitrogen atom of the ligand in complex formations with any of the metal ions. Disappearance of the  $\nu\text{OH}$  (phenolic) band of the ligand (3169  $\text{cm}^{-1}$ ) peak size and/or appearance of new band(s) of  $\nu\text{C}-\text{O}$  (phenolic

**Table 6.**  $^1\text{H}$  and  $^{13}\text{C}$  NMR spectral data for ligand and its metal complexes.

Compounds	$\delta$ (ppm)	$^1\text{H}$ NMR assignment	$\delta$ (ppm)	$^{13}\text{C}$ NMR assignment
$\text{C}_9\text{H}_8\text{O}_2\text{N}_2\text{S}$	3.85	Methylene ( $\text{CH}_2\text{-S}$ )	31.5	Aliphatic $\text{CH}_2\text{ S}$
	6.7-7.9	Aromatic H	119-125	Aromatic C
	10	Imine H ( $=\text{NH}$ )	126.5	Phenolic C( $\text{C-OH}$ )
	6.78	Phenolic H( $-\text{OH}$ )	148	Imine C( $\text{C=NH}$ )
			167.9	Carbonyl C( $\text{C=O}$ )
[Zn- $\text{L}_4$ ]	3.85	Methylene ( $\text{CH}_2\text{-S}$ )	42.90	Aliphatic $\text{CH}_2\text{ S}$
	6.7-7.9 and 9.5	Aromatic H	115.82-125	Aromatic C
			126.5	Phenolic C( $\text{C-OH}$ )
			151.2	Imine C( $\text{C=NH}$ )
			167.4	Carbonyl C( $\text{C=O}$ )
[Cd- $\text{L}_4$ ]	3.85	Methylene ( $\text{CH}_2\text{-S}$ )	42.91	Aliphatic $\text{CH}_2\text{ S}$
	6.7-7.85 and 9.4	Aromatic H	115.78-125	Aromatic C
			126.45	Phenolic C( $\text{C-OH}$ )
			149	Imine C( $\text{C=NH}$ )
			167.45	Carbonyl C( $\text{C=O}$ )
[Hg- $\text{L}_2$ ]	3.85	Methylene ( $\text{CH}_2\text{-S}$ )	42.92	Aliphatic $\text{CH}_2\text{ S}$
	6.75-7.85 and 9.4	Aromatic H	115.8-125	Aromatic C
			126.50	Phenolic C( $\text{C-OH}$ )
			147.5	Imine C( $\text{C=N}$ )
			167.41	Carbonyl C( $\text{C=O}$ )

L= 3-(2-hydroxyphenyl)-2-iminothiazolidin-4-one.

group) on complexation, and the appearance of new band at  $587\text{ cm}^{-1}$  for [Zn- $\text{L}_4$ ] complex and at  $578\text{ cm}^{-1}$  in [Cd- $\text{L}_4$ ] complex can be due to  $\nu(\text{M-O})$  band. This indicate the formation of  $\nu(\text{M-O})$  band. The other new bands appearing at  $446$  and  $541\text{ cm}^{-1}$  in the Hg complex can also substantiate the formation of  $\nu(\text{M-O})$  and  $\nu(\text{M-N})$ , respectively. These shifts of absorption bands to lower wave numbers in the complexes, strongly suggest the possible coordination of the heterocyclic nitrogen and phenolic oxygen to the metal centers. Infrared spectral studies clearly reveal that binding modes of the ligand is through deprotonated phenolic oxygen and heterocyclic nitrogen atoms and there is no role of anions from the  $\text{M}^{2+}$  salts in the inner coordination spheres of the complexes.

Therefore the ligand behaves as a neutral bidentate ligand coordinated, to Hg (II) ions, through the nitrogen atoms of the ring, and oxygen atoms of the phenolic groups to give a four membered chelate ring complexes (Viñuelas-Zahinos et al., 2011). However, the ligand acting as monodentate coordinating through phenolic oxygen in case of Zn(II) and Cd(II) complexes.

### NMR ( $^1\text{H}$ and $^{13}\text{C}$ ) spectra analysis

The  $^1\text{H}$ NMR and  $^{13}\text{C}$ NMR data of the 3-(2-hydroxyphenyl)-2-iminothiazolidin-4-one ligand and its complexes recorded in DMSO solvent as shown on Table 6. The  $^1\text{H}$

NMR spectral data (Table 6) of 3-(2-hydroxyphenyl)-2-iminothiazolidin-4-one displayed chemical shifts at  $\delta 3.85$  is attributed to heterocyclic (2H) between carbonyl group and heterocyclic sulfur, at  $\delta 10$  to imine (1H), at  $\delta 6.7-7.9$  and  $9.45$  to benzene ring (4H) and at  $\delta 6.78$  corresponding to phenolic (1H). On the other hands, the  $^{13}\text{C}$  NMR spectrum displays the aliphatic  $\text{CH}_2\text{-S}$  band at  $\delta 31.5$ , the HC (aromatic ring) band in the range (119-125), phenolic C( $\text{C-OH}$ ) band at  $\delta 126.5$ , imine C( $\text{C=NH}$ ) band at  $\delta 148$  Carbonyl C( $\text{C=O}$ ) display band at  $\delta 167.9$ .

As indicated in  $^1\text{H}$  and  $^{13}\text{C}$  NMR spectral data of the ligand and its complexes, the changes with each chemical shift for the complexes were the same as the ligand. However, in the  $^1\text{H}$  NMR spectra of [Zn- $\text{L}_4$ ] and [Cd- $\text{L}_4$ ] complexes absence shifts at  $\delta 10$  were attributed to imine hydrogen. Whereas there was no  $^1\text{H}$  spectra shifts of [Hg- $\text{L}_2$ ] at  $\delta 10$  attributed to imine (1H) and  $\delta 6.78$  substantiate a phenolic H( $-\text{OH}$ ). Therefore, these results of  $^1\text{H}$  and  $^{13}\text{C}$  NMR analyses for the ligand and its complexes also support the inferences made based on the IR regarding the structure of 3-(2-hydroxyphenyl)-2-iminothiazolidin-4-one and its [Zn- $\text{L}_4$ ], [Cd- $\text{L}_4$ ] and [Hg- $\text{L}_2$ ] complexes.

### Conductivity measurements

Complexes prepared in this work showed molar

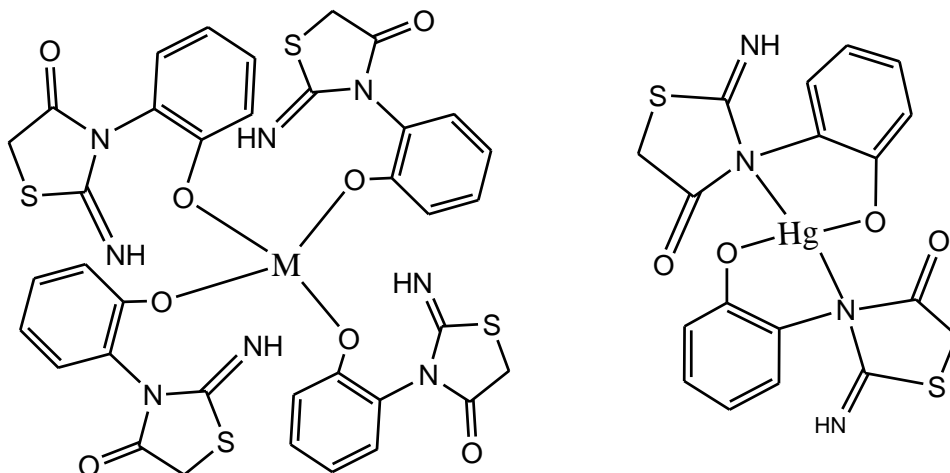


**Figure 4.** The proposed structural formula of [Zn-L<sub>4</sub>], [Cd-L<sub>4</sub>] and [Hg-L<sub>2</sub>] complexes with 3-(2-hydroxyphenyl)-2-iminothiazolidin-4-one ligand. M is Zn(II) and Cd(II).

conductance with values of 133, 125 and 122  $\mu\text{Smol}^{-1}\text{cm}^2$  for [Zn-L<sub>4</sub>], [Cd-L<sub>4</sub>] and [Hg-L<sub>2</sub>], respectively (all measured in DMSO at room temperature). These values indicate high conductivity nature of the complexes, and the molar conductance values suggested that all the complexes are electrolytes.

### Proposed structures of the synthesized complexes

Based on the inferences made from C, H, N, S and metals analyses, chloride test, conductometric, IR spectroscopy and UV/Vis or electronic spectral studies, the following general structures can be proposed for [Zn-L<sub>4</sub>], [Cd-L<sub>4</sub>] and [Hg-L<sub>2</sub>] complexes with the ligand, L, being, 3-(2-hydroxyphenyl)-2-iminothiazolidin-4-one, as presented in Figure 4.

### Conclusion

This paper reports spectrophotometric study of the metal complex of Zn<sup>2+</sup>, Cd<sup>2+</sup>, and Hg<sup>2+</sup> with heterocyclic ligand of 3-(2-hydroxyphenyl)-2-iminothiazolidin-4-one. The stoichiometric studies showed that there is a similar pattern in the optical density or absorbance of each of these complexes showing similar specific values at two temperatures giving rise to 1:4, 1:4 and 1:2 metals to ligand ratios in the complexes of [Zn-L<sub>4</sub>], [Cd-L<sub>4</sub>] and [Hg-L<sub>2</sub>], respectively. The metal-ligand complex stability constants (K<sub>s</sub> values) have been found to be in the order: [Zn-L<sub>4</sub>] > [Cd-L<sub>4</sub>] > [Hg-L<sub>2</sub>]. This order is found to be in good agreement with the Irving-Williams order of stability for divalent metal ion complexes. The conductometric study indicates the electrolytic nature of all synthesized complexes. All complexes were formulated as

mononuclear compounds involving 1:4 for Zn<sup>2+</sup> and Cd<sup>2+</sup> whereas Hg<sup>2+</sup> complex shows 1:2 metal to ligand ratio derived from elemental and metal analyses. Based on the infrared results, it is concluded that the ligand behaves as a neutral bidentate ligand coordinated to the metal ions through the nitrogen atoms of heterocyclic groups, and oxygen atoms of the phenolic groups to give a chelating complexes. <sup>1</sup>H and <sup>13</sup>C NMR justified theoretically proposed structure of complexes from their stoichiometry. Magnetic studies indicated four coordinate tetrahedral geometry of [Hg-L<sub>2</sub>] and distorted geometries of [Zn-L<sub>4</sub>], [Cd-L<sub>4</sub>] complexes having a charge transfer transitions. The values of stability constants and negative sign of free energy changes of the complexes in the solvent used indicate that metal-ligand reactions are spontaneous and complexes are stable at room temperatures. Stability constant results suggest that ligand used is a good chelating agent for all the three metals.

### Conflict of Interest

The authors have not declared any conflict of interest

### REFERENCES

- Andres CJ, Bronson JJ, D'Andrea SV (2000). 4-Thiazolidinones: Novel inhibitors of the bacterial enzyme MurB. *Bioorg. Med. Chem. Lett.* 10(8):715–717.
- Barreca ML, Chimirri A, De Luca L, Monforte AM, Monforte P, Rao A, Zappala M, Balzarini J, De Clercq E, Pannecouque C, Witvrouw M (2001). Discovery of 2,3-diaryl-1,3-thiazolidin-4-ones as potent anti-HIV-1 agents. *Bioorg. Med. Chem. Lett.* 11(13):1793–1796.
- Brown FC (1961). 4-Thiazolidinones. *Chem. Rev.* 61:463–521.
- Diurno MV, Mazzoni O, Piscopo E, Calignano A, Giordano F, Bolognese A (1992). Synthesis and antihistaminic activity of some thiazolidin-4-ones. *J. Med. Chem.* 35(15):2910–2912.
- Harvey AE, Manning DL (1950). Spectrophotometric methods of

- establishing empirical formulas of colored complexes in solution. *J. Am. Chem. Soc.* 72:4488-4493.
- Look GC, Schullek JR, Holmes CP, Chinn JP, Gordon EM, Gallop MA (1996). The identification of cyclooxygenase-1 inhibitors from 4-thiazolidinone combinatorial libraries. *Bioorg. Med. Chem. Lett.* 6(6):707-712.
- Mulwad VV, Choudhari BP (2005). Synthesis and antimicrobial screening of N[*coumarin-6-ylamino*] thiazolidinone and spiroindolthiazolidinone derivatives. *Indian J. Chem.* 44:1074-1083
- Pulici M, Quartieri F (2005). Traceless solid-phase synthesis of 2-amino-5-alkylidene-thiazol-4-ones. *Tetrahedron Lett.* 46(14):2387-2391.
- Singh SP, Parmar SS, Raman K, Stenberg VI (1981). Chemistry and biological activity of thiazolidinones. *Chem. Rev.* 81:175-203.
- Suresh MS, Prakash V (2010). Preparation and characterization of Cr(III), Mn(II), Co(III), Ni(II), Cu(II), Zn(II) and Cd(II) chelates of schiffs base derived from vanillin and 4-amino antipyrine. *Int. J. Phys. Sci.* 5(14):2203-2211
- Viñuelas-Zahinos E, Luna-Giles F, Torres-García P, Rodríguez AB, Bernalte-García A (2011). Effects of a derivative thiazoline/thiazolidine azine ligand and its cadmium complexes on phagocytic activity by human neutrophils. *Inorganica Chimica Acta.* 366:373-379.
- Vosburgh WC, Cooper GR (1941). The identification of complex ions in solution by spectrometric measurements. *J. Am. Chem. Soc.* 63:437-442.

*Full Length Research Paper*

# Thermodynamic analysis of some volatile species at elevated pressure and temperature during combustion of Pakistani Lakhra and Thar lignite chars

Gul-e-Rana Jaffri<sup>1\*</sup>, Syed Ali Rizwan shah Jaffri<sup>2</sup> and Syed Ali Rehan Shah Jaffri<sup>3</sup>

<sup>1</sup>Fuel Research Centre, PCSIR, Off University Road Karachi-75280, Pakistan.

<sup>2</sup>Wuhan University of Science and Technology, China.

<sup>3</sup>IRAO, Federal Board of Revenue, Islamabad, Pakistan.

Received 30 April, 2015; Accepted 17 August, 2015

Volatile species (e.g. Na-,K-,Cl-, and S) are released during thermal conversion of coal causing eventual problems such as fouling, slagging and corrosion, especially in gas turbines, on super heaters and in the colder part of heat recovery systems. Thermodynamic study of the released inorganic compounds is supportive before eventually launching experimental work. Therefore, thermodynamic equilibrium was calculated using FactSage 5.2, simulating combustion conditions at elevated pressure (5, 10 and 15 bar) and elevated temperature (1000, 1400 and 1600°C). Their releasing order of various volatile species was estimated by plotting mole fraction of each species at temperature 1000°C and pressure 1 bar. These calculations predict that SO<sub>2</sub> is the most stable species for combustion. At all pressure the lowest amount of NaCl and KCl volatilized for LKH and THR lignite char. Evolution of NaCl, KCl and HCl depends on the amount of Cl present in both lignite chars.

**Key words:** Combustion, fact sage, equilibrium calculations, release of volatile species.

## INTRODUCTION

Pakistan is abundant natural coal reserves in Sindh, Punjab, Baluchistan, Northwest frontier province and has 33.0 trillion tons world third largest resources in south-eastern part of the country that is, Thar (Final USAID-Pakistan circular Debt Report-2013). Generally, the electricity generation from coal is economical and cost competitive. Worldwide, approximately 41% energy is producing through coal but Pakistan despite of huge coal resources only 0.1% of its power is produces through coal and severe energy crises is raising every year

(Usmani, 2014) but maximum efficiency may be achieved by reforms the existing and installation of additional power plants (The News, 2013)

Pakistani Lakhra and Thar lignite's due to low ash, high moisture, volatility and Sulphur need some special techniques for their utilization in combustion, gasification and power generation. The efficiency of power generation may reduce by high moisture moreover the presence of ash is responsible for slugging and fouling problem in conventional boiler.

\*Corresponding author. E-mail: [jaffri\\_gul@yahoo.com](mailto:jaffri_gul@yahoo.com). Tel: 92-3153862290.

Author(s) agree that this article remain permanently open access under the terms of the [Creative Commons Attribution License 4.0 International License](https://creativecommons.org/licenses/by/4.0/)

**Table 1.** Proximate and ultimate analysis of Pakistani LKH and THR lignite and char.

Coal type	Proximate analysis					Ultimate analysis			
	M <sub>ad</sub> %	A <sub>ad</sub> %	V <sub>ad</sub> %	FC <sub>ad</sub> %	S <sub>t,ad</sub> %	H <sub>ad</sub> %	C <sub>ad</sub> %	N <sub>ad</sub> %	O <sub>ad</sub> %
LKH lignite	10.24	14.66	44.54	30.56	5.15	3.07	52.44	0.85	13.6
THR lignite	8.5	19.37	48.52	23.66	4.02	2.94	49.93	0.98	14.31
LKH lignite char	6.07	28.19	4.82	60.92	5.62	1.71	54.77	0.89	2.75
THR lignite char	3.88	36.25	6.18	53.69	3.46	1.36	51.78	0.74	2.53

$$O_{ad}\% = 100 - A_{ad}\% - S_{t,ad}\% - C_{ad}\% - H_{ad}\% - N_{ad}\% - M_{ad}\%.$$

**Table 2.** The ash composition and fusion temperature of Pakistan chars.

Char sort		LKH char	THR char
A <sub>ad</sub> %		28.19	36.25
Ash  Composition analysis of ash, %	SiO <sub>2</sub> / Al <sub>2</sub> O <sub>3</sub>	1.32	2.13
	SiO <sub>2</sub>	27.98	39.01
	Al <sub>2</sub> O <sub>3</sub>	21.21	18.31
	Fe <sub>2</sub> O <sub>3</sub>	24.85	22.46
	CaO	9.44	9.82
	MgO	4.77	2.66
	TiO <sub>2</sub>	1.53	1.95
	SO <sub>3</sub>	8.08	4.10
	K <sub>2</sub> O	0.15	0.05
	Na <sub>2</sub> O	1.16	0.96
	P <sub>2</sub> O <sub>5</sub>	0.53	0.32
Fusion temperature t/°C	DT	1228	1188
	ST	1234	1216
	FD	1239	1226

Unfortunately during combustion at high temperature and pressure, highly volatile species (Na, K, Cl and S) released and penetrate in hot gas filtration unit and gas turbine blades. The power plant efficiency may be achieved by hot gas cleaning (Blacing et al., 2011)

Therefore the comprehensive knowledge of released volatile species during combustion at elevated temperature and pressure is required prior to carry out experiment by utilization of Pakistani lignite chars.

Thermodynamic equilibrium calculations is the basis for obtaining such information and its method is capable of identifying species that are stable only at high temperature especially those employed in commercial combustors. The results are useful guidance for predicting the trends occurring during Combustion.

Therefore the present study simulates the combustion at high pressure (5 to 15) bar at 1000°C and Temperature (1000 to 1600°C) at 1 bar pressure and also predicts the release of volatile species for Pakistani Lakhra and Thar lignite chars using equilibrium calculations by Fact sage 5.2.

## MATERIALS AND METHODS

Two kinds of Pakistani THR and LKH lignite from Fuel Research Center, PCSIR, Karachi, Pakistan, are mainly used. Their proximate and ultimate analysis is given in Table 1. Char was made by following procedure. Firstly, the 60 or 76.06 g by weight of raw THR or LKH coal was loaded twice with some ceramic beads in fixed bed inserted in an electric furnace with sufficient heat and it underwent a carbonization in nitrogen atmosphere under temperature 750°C and ambient pressure with heating rate 15°C/min and flow rate 664.675 L/h for one hour. Then these chars removed from ceramic beads were respectively pulverized with particle size 0-0.154 mm (< 100 mesh). The composition of the above chars and ashes are listed respectively in Table 1 and 2. The chemical composition of Pakistani chars is included in Table 3.

### Calculation procedure

Thermodynamic equilibrium calculations were performed using Fact sage 5.2. The initial model composition is based on the data of elementary and chemical composition relate to 1 g of lignite char. The thirteen elements C, H, N, S, O, Cl, Al, Ca, Fe, K, Mg, Na and Si were included in the computation, as listed in Table 1 and 3.

The results were calculated by plotting mole fraction of each



**Table 3.** Chemical composition of Pakistani Chars %.

Coal type	Si	Al	Fe	Ca	Mg	Ti	K	Na	P	Cl
LKH lignite Char	3.69	1.58	2.45	1.90	0.812	0.26	0.031	0.12	0.042	0.000012
THR lignite Char	6.61	1.76	2.83	2.55	0.58	0.42	0.015	0.131	0.033	0.000015

**Table 4.** Calculated mole fraction at pressure 5 to 15 bar and temperature 1000°C for combustion.

Alkali species	Mole fraction		
	P (bar)	LKH Char	THR Char
SO <sub>2</sub>	5	4.4577E-03	2.1378E-03
	10	4.1044E-03	1.7095E-03
	15	3.9034E-03	1.4847E-03
H <sub>2</sub> S	5	7.4243E-04	8.2583E-04
	10	9.5193E-04	8.3085E-04
	15	9.7031E-04	8.3337E-04
NaCl	5	3.8999E-10	1.0407E-09
	10	2.7925E-10	7.5006E-10
	15	2.2892E-10	6.1761E-10
KCl	5	1.0250E-10	2.7352E-10
	10	7.3394E-11	1.9713E-10
	15	6.0164E-11	1.6232E-10
HCl	5	1.2920E-08	1.6933E-08
	10	1.3064E-08	1.7311E-08
	15	1.3132E-08	1.7484E-08

species vs Pressure (5 to 15 bar) at 1000°C and Temperature (1000 to 1600°C) at 1 bar pressure for combustion process as shown in Figure 1 to 10 and calculated mole fractions are listed in Table 4 and 5.

#### Definition of conditions

To simulate the condition of combustion of LKH lignite Char excess air, O<sub>2</sub>=1.6733 g or (167.33%) and N<sub>2</sub>= 5.5085 g or (550.85%) and for THR lignite char excess air, O<sub>2</sub>=1.5411 g or (154.11%) and N<sub>2</sub>= 5.0733 g or (507.33%) was added to system.

## RESULTS AND DISCUSSION

### Release of volatile species during high pressure combustion

The computed release of SO<sub>2</sub>, H<sub>2</sub>S, NaCl, KCl and HCl under pressurized combustion is listed in Table 4. On the basis of the calculated mole fraction the release of SO<sub>2</sub> gradually decreases with increasing the pressure from 5 to 15 bar, as shown in Figure 1, but higher than H<sub>2</sub>S due to higher combustion product while release of H<sub>2</sub>S

gradually increases with increasing pressure during combustion, as indicated in Figure 2. Such changes are mainly as a consequence of the Le Chatelier-van't Hoff Law.

Therefore, lower release of SO<sub>2</sub> to the gas phase occurs for THR Char and even a sharp decrease was observed at 15 bar. The release of H<sub>2</sub>S is showing little higher at 15 bar for LKH char.

The results of NaCl and KCl are depicted in Figures 3 and 4. The release of NaCl, KCl strongly decreases with increasing pressure from 5 to 15 bar for LKH and THR char. The sharp decrease of NaCl, KCl was observed in LKH char at 15 bar.

The release of HCl gradually increases with increasing pressure 5 to 15 bar for LKH and THR char as obviously indicated in Figure 5. The sharp increase in mole fraction of THR char was observed at 15 bar. The decrease and increase volatilization in LKH and THR Char may be lower content of Cl in LKH Char and little high content in THR Char but the system is in equilibrium and no effect on reaction will takes place because no of moles of the gas are same on each side of chemical equation of NaCl, KCl and HCl (Lechatelier Principle).

**Table 5.** Calculated mole fraction at Temperature 1000 to 1600°C and pressure 1 bar for combustion.

Alkali species	Mole fraction		
	T°C	LKH Char	THR Char
SO <sub>2</sub>	1000	5.3452E-03	3.0045E-03
	1400	6.8794E-03	4.5989E-03
	1600	6.8702E-03	4.5924E-03
H <sub>2</sub> S	1000	3.6219E-04	4.0719E-04
	1400	9.6130E-07	1.0933E-06
	1600	9.0319E-08	1.0107E-07
NaCl	1000	8.3226E-10	2.1296E-09
	1400	7.3976E-09	1.1463E-08
	1600	7.7522E-09	1.2331E-08
KCl	1000	2.1874E-10	5.5969E-10
	1400	1.5397E-09	2.3062E-09
	1600	2.7221E-09	3.1470E-09
HCl	1000	1.2352E-08	1.5544E-08
	1400	4.4385E-09	4.4303E-09
	1600	2.8599E-09	2.6839E-09

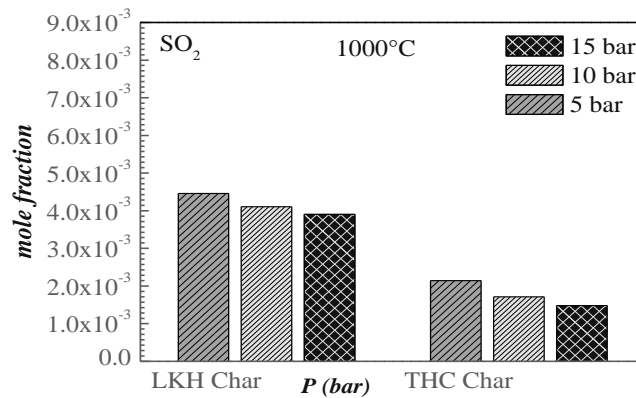


**Figure 1.** Predicted results of SO<sub>2</sub> at high pressure combustion.

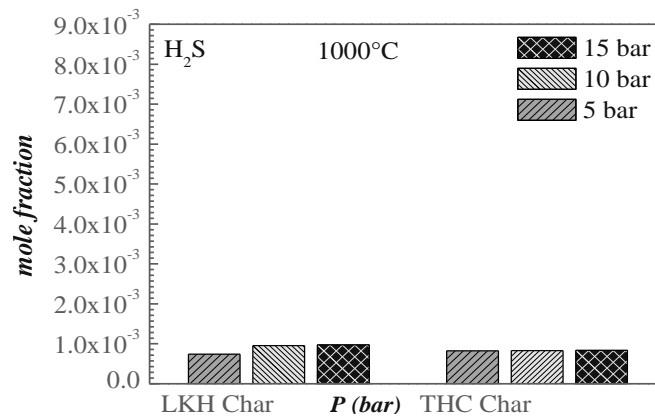


**Figure 2.** Predicted results of H<sub>2</sub>S at high pressure combustion.

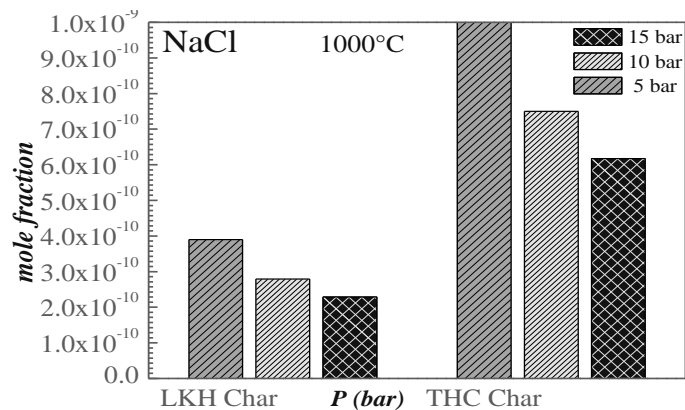


Figure 3. Predicted results of NaCl at high pressure combustion.

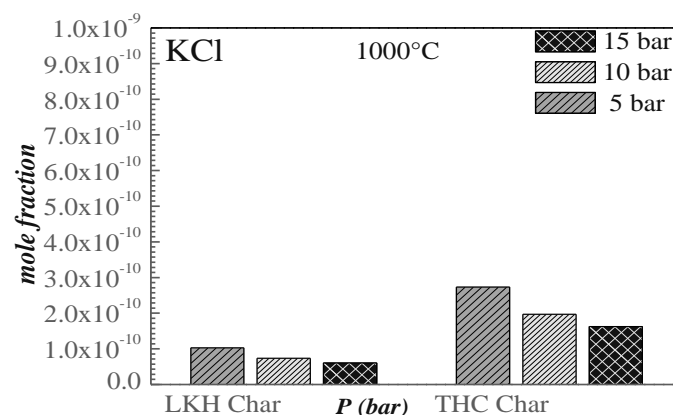


Figure 4. Predicted results of KCl at high pressure combustion.

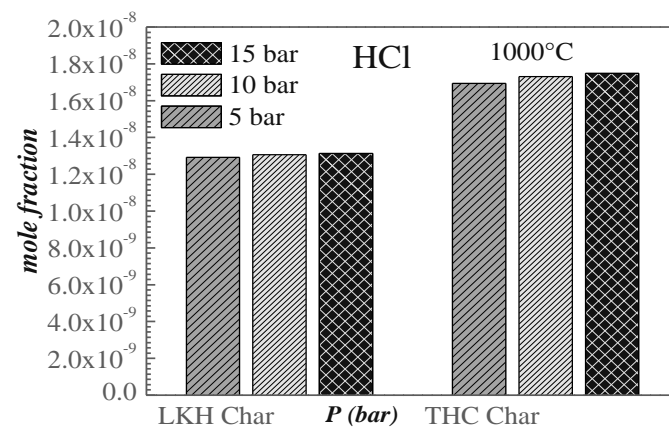
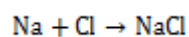
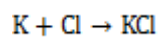


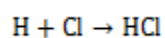
Figure 5. Predicted results of HCl at high pressure combustion.



(1) **Release of volatile species during high temperature combustion**



(2)



(3)

The predicted results concerning the release of  $\text{SO}_2$ ,  $\text{H}_2\text{S}$ ,  $\text{NaCl}$ ,  $\text{KCl}$  and  $\text{HCl}$  under high temperature combustion

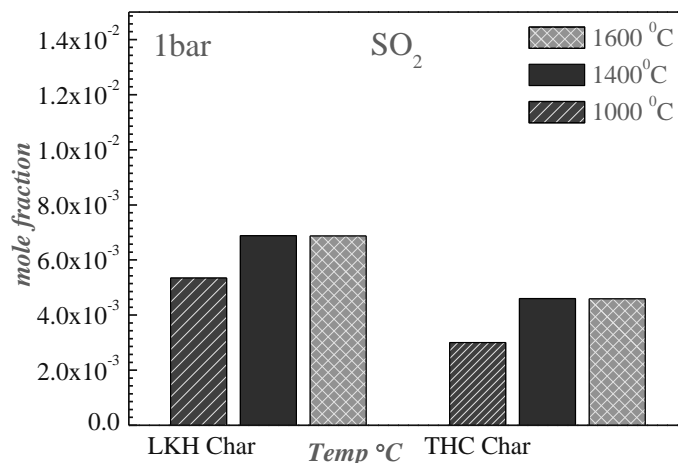


Figure 6. Predicted results of SO<sub>2</sub> at high pressure combustion.

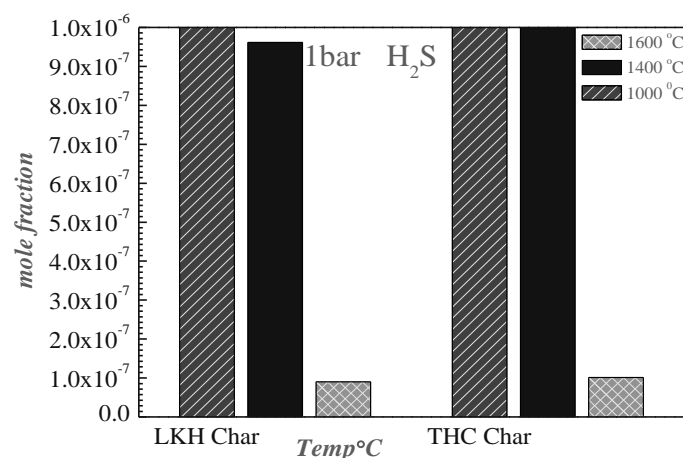


Figure 7. Predicted results of H<sub>2</sub>S at high temperature combustion.

are listed in Table 5. Figure 6, consider the mole fraction as the base for release of SO<sub>2</sub> for two samples: It gradually increases with increasing temperature 1400 to 1600°C for LKH and THR char may be the exothermic formation of SO<sub>2</sub> is shifting equilibrium right side for complete formation of SO<sub>2</sub> reaction so volatilization of SO<sub>2</sub> is observed higher at 1400°C (Lechatelier Principle). The predicted results of H<sub>2</sub>S are depicted in Figure 7. It strongly decreases with increasing temperature for both LKH and THR char may be decrease in volatilization of H<sub>2</sub>S is shifting the equilibrium to the left therefore strong decreased is observed for LKH char at 1600°C (Lechatelier Principle).

The release of NaCl and KCl is increasing with increases of temperature as clearly indicated in Figures 8 and 9. The high release of NaCl and KCl is observed at 1600°C for THR char and this may be due to the fact that in thermodynamic equilibrium system the influence of

high temperature increases the partial pressure of the species so volatilization increases (Broström, 2010). The predicted results of HCl are shown in Figure 10. The release of HCl decreases with increasing temperature and this strong decrease HCl is observed for THR char at 1600°C may be because of the equilibrium shifts to the left, decreases the volatilization of HCl. (Chemical Equilibria)

#### Comparison of predicted combustion results at elevated pressure with high temperature

Thermodynamic equilibrium calculations were used to compare the predicted results of combustion both elevated pressure and temperature. The comparison of predicted combustion results at elevated pressure with high temperature as shown in Figure 11. It is found that

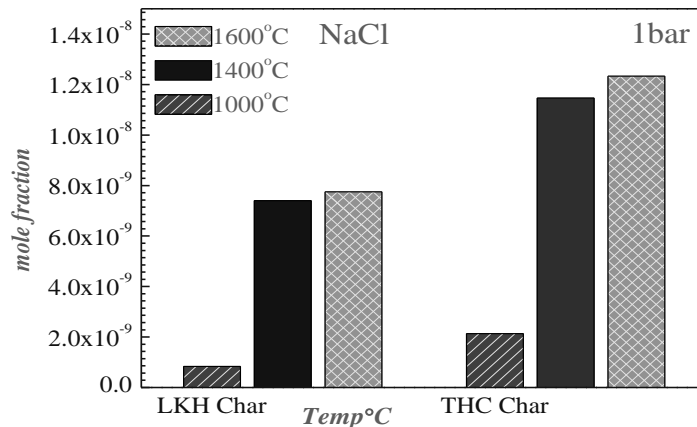


Figure 8. Predicted results of NaCl at high temperature combustion.

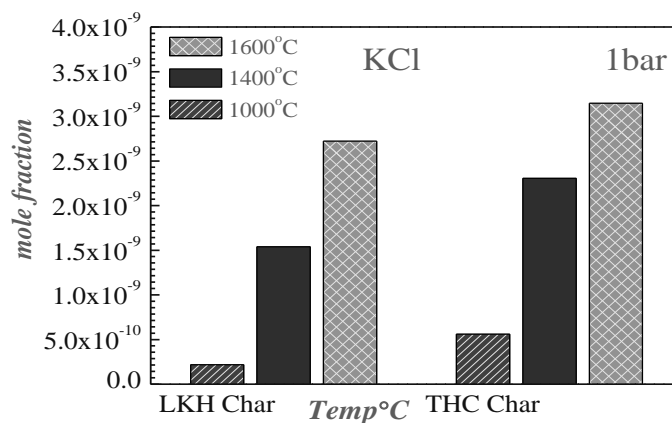


Figure 9. Predicted results of KCl at high temperature combustion.

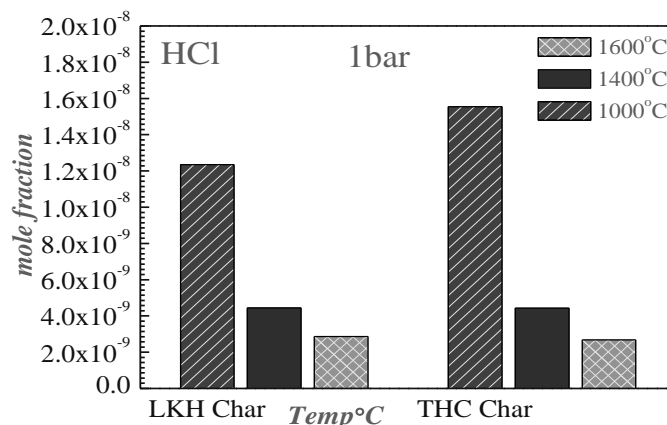
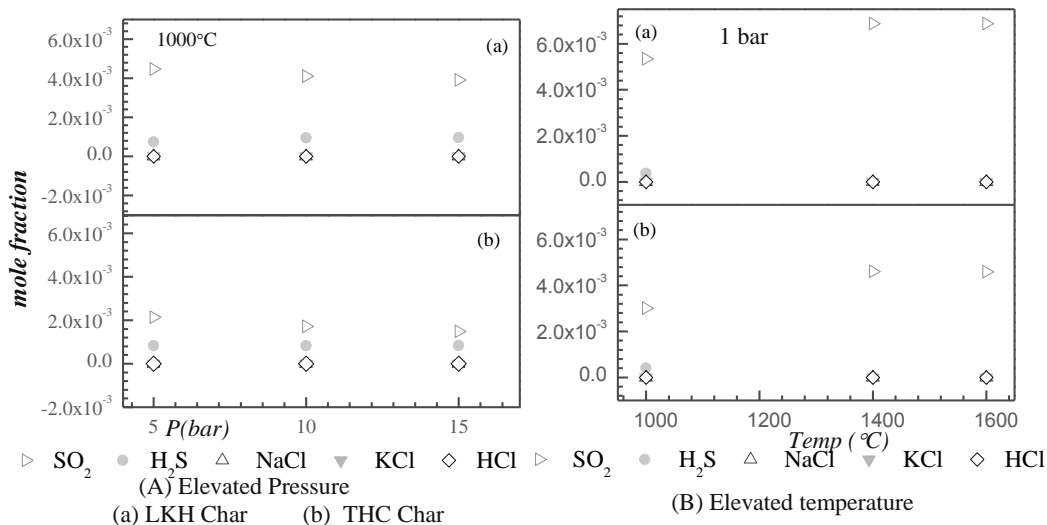


Figure 10. Predicted results of HCl at high temperature combustion.

the release of SO<sub>2</sub> is very sharply reached at maximum value for LKH char at 1400°C in Figure 11(B),(a), as compared to pressure 5 bar for LKH char in Figure 11 Aa moreover also greater than the release of H<sub>2</sub>S, NaCl, KCl

and HCl at elevated pressure.

On the basis of calculated mole fractions, the order of release species SO<sub>2</sub>, H<sub>2</sub>S, NaCl, KCl and HCl for LKH and THR lignite char during combustion at elevated



**Figure 11.** Comparison of predicted equilibrium calculation results of combustion at elevated pressure and temperature.

temperature and pressure are predicted as follows:

1. Releasing order of species at elevated temperature:

LKH char ( $\text{SO}_2 > \text{H}_2\text{S} > \text{NaCl} > \text{KCl} < \text{HCl}$ )  
 THC Char ( $\text{SO}_2 > \text{H}_2\text{S} > \text{NaCl} > \text{KCl} < \text{HCl}$ )

2. Releasing order of species at elevated pressure:

LKH Char ( $\text{SO}_2 > \text{H}_2\text{S} > \text{NaCl} > \text{KCl} < \text{HCl}$ )  
 THC Char ( $\text{SO}_2 > \text{H}_2\text{S} > \text{NaCl} > \text{KCl} < \text{HCl}$ )

On the basis of releasing order, the  $\text{SO}_2$  release is higher at elevated temperature than elevated pressure. The release of  $\text{SO}_2$  is highest for LKH char at  $1400^\circ\text{C}$  and lowest for THC char at 15 bar, the order of release at elevated temperature and elevated pressure is LKH Char  $>$  THC Char.

For  $\text{H}_2\text{S}$  the higher and lower release is observed for LKH char at 15 and 5 bar. The order of release is LKH char  $>$  THC char at elevated pressure and elevated temperature is THC char  $>$  LKH char. The NaCl release is higher for THR Char at  $1600^\circ\text{C}$  and lower for LKH char at  $1000^\circ\text{C}$  than elevated pressure. The order of release at elevated temperature and elevated pressure is THC char  $>$  LKH char.

The KCl release is higher for THR char at  $1600^\circ\text{C}$  and lower for LKH char at  $1000^\circ\text{C}$  than elevated pressure, the order of release is THR char  $>$  LKH char. The order of release at elevated temperature and elevated pressure is THC char  $>$  LKH Char.

The HCl release is higher for THR char at 15 bar and lower at 5 bar for LKH char than elevated temperature, the order of release is THR char  $>$  LKH char. The order of release at elevated temperature is LKH char  $>$  THR char

## Conclusion

1. The high volatilization of  $\text{SO}_2$  for both at elevated temperature and pressure can be predicted that  $\text{SO}_2$  is the most stable specie for combustion.
2. The volatilization of  $\text{SO}_2$  is predicted higher for LKH char ( $1400^\circ\text{C}$ ) at elevated temperature and lowers for THC char (15bar) at elevated pressure during combustion.
3. The volatilization of  $\text{H}_2\text{S}$  is predicted higher for LKH char (15 bar) at elevated pressure and lowers for LKH Char ( $1600^\circ\text{C}$ ) at elevated temperature.
4. The release order of NaCl, KCl and HCl species at elevated pressure is not similar with elevated temperature. The predicted release of NaCl, KCl is higher for LKH and THC char at elevated temperature and while volatilization of HCl for LKH and THC char is higher at elevated pressure.
5. The volatilization of NaCl, KCl and HCl is dependent on Cl content present in the LKh and THR Char.

## Conflict of Interest


The authors have not declared any conflict of interest.

## REFERENCES

- An overview of Paksitan Energy Sector Report by Islamabad Chamber of Commerce & Industry (ICCI), The News, (2013). <https://www.scribd.com/doc/.../Pakistan-Energy-Crisis-an-Overview> Dec 7, 2013
- Blacing M, Muller M (2011). Influence of pressure on release of inorganic species during high temperature gasification of coal. J. Fuel. 90:2326-2333. <http://dx.doi.org/10.1016/j.fuel.2011.02.013>
- Broström M (2010). "Aspects of alkali chloride chemistry on deposit

formation and high temperature corrosion in biomass and waste fired boilers". Academic dissertation, Energy Technology and Thermal Process Chemistry Umeå University Sweden. <http://www.diva-portal.org/smash/get/diva2.../FULLTEXT01.pdf> MarkusMark...  
Chemical Equilibria <http://pages.towson.edu/ladon/chemeq.html>  
Final USAID-Pakistan circular Debt Report (2013). [http://www.pc.gov.pk/.../2013/Final\\_USAID-Pakistan](http://www.pc.gov.pk/.../2013/Final_USAID-Pakistan)  
Le Chatelier 'S principle <https://www.chemguide.co.uk/physical/equilibria/lechatelier.html>

Usmani FS, (2014). Pakistan facing energy crisis. <http://www.dawn.com/news/1130945>



# African Journal of Pure and Applied Chemistry

## Related Journals Published by Academic Journals

- *African Journal of Mathematics and Computer Science Research*
- *International Journal of the Physical Sciences*
- *Journal of Geology and Mining Research Technology*
- *Journal of Environmental Chemistry and Ecotoxicology*
- *Journal of Internet and Information Systems*
- *Journal of Oceanography and Marine Science*
- *Journal of Petroleum Technology and Alternative Fuels*

**academicJournals**